

Online Appendix of:
A Congestion Theory of Unemployment Fluctuations
Yusuf Mercan, Benjamin Schoefer and Petr Sedláček

Contents

List of Tables	2
List of Figures	2
A Empirical Appendix: Construction of Worker Flows and Transition Probabilities, and Robustness	3
B Robustness: Job-to-Job Transitions and Total Hires	16
C Further Details on Identification of Congestion	21
D A Generalization of the Baseline Model: Types vs. Inputs	26
E Solution Method	27
F Details of the Baseline Parameterization: Homogeneous Steady State Marginal Products Across Types	29
G Alternative Calibration: Small Surplus/"High b "	30
H Robustness of Model Performance to the Number of Worker Types	33
I Business Cycle Statistics Including Full Correlation Matrices	36
J Alternative Calibration: Accounting for Labor Force Participation and Matching EU Flows	39
K Deriving the Iso-congestion Curve	43
L Alternative Mechanism: Convex Hiring Costs	46
M Historical Decomposition: Additional Material	48
Bibliography	51

List of Tables

A1	Discrete vs. Time-Aggregation Adjusted Worker Transitions	6
A2	Business Cycle Properties: Alternative Smoothing Parameter	11
A3	Benchmarks: Elasticity of Substitution Parameters Estimated in the Literature	22
A4	Separation Shocks and Other Disturbances: Adjusted R-squared	24
A5	Business Cycle Properties: No-Congestion, Low-Surplus Model	32
A6	Business Cycle Properties in the Data	36
A7	Business Cycle Properties in the No-Congestion Model without Separation Shocks	36
A8	Business Cycle Properties in the No-Congestion Model with Separation Shocks	37
A9	Business Cycle Properties in the Congestion Model—Baseline (Matching UE/E)	37
A10	Business Cycle Properties in the Congestion Model—Robustness (Matching EU & Participation)	38
A11	Business Cycle Properties in the Congestion Model—Robustness (Matching EU only)	38
A12	Business Cycle Properties: Convex Hiring Cost Model	47
A13	Historical Decomposition of Unemployment: Model and Counterfactuals	50

List of Figures

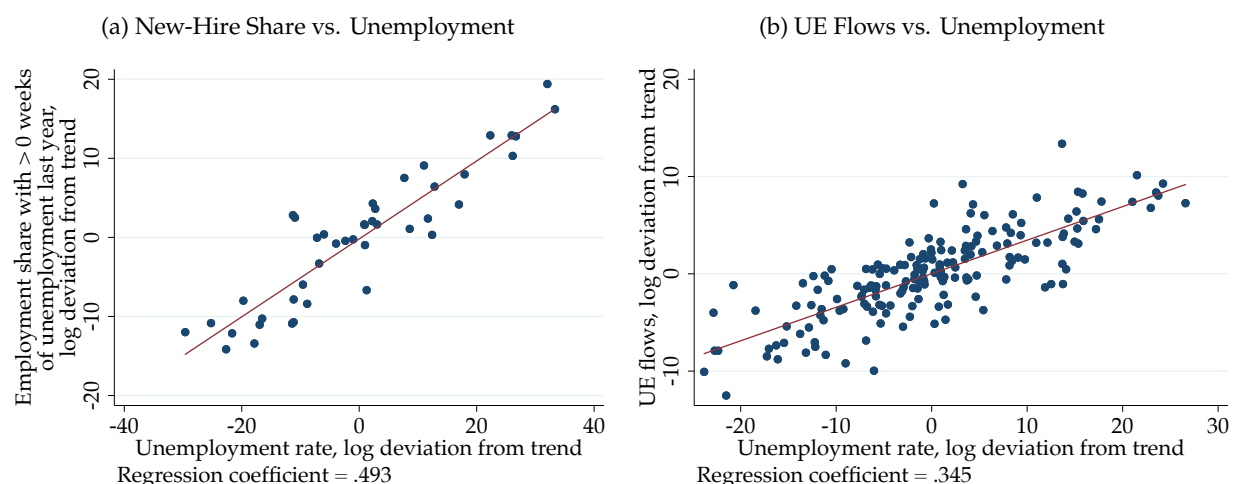
A1	The Countercyclicality of Hiring out of Unemployment: Okun’s Laws and Elasticities	3
A2	Comparing Discrete and Time Aggregation Adjusted UE Flows	7
A3	Comparing Discrete and Time Aggregation Adjusted Flow Probabilities	8
A4	Comparing Discrete and Time Aggregation Adjusted UE Flows (Shimer 2012)	9
A5	Countercyclicality of the Employment Share with Nonemployment Past Year	10
A6	The Countercyclicality of New Hire Share: CPS Worker Flows	11
A7	Cyclicality of Share of New Hires in Employment: CPS Worker Flows	12
A8	Cyclicality of New Hires: CPS Worker Flows	13
A9	The Countercyclicality of Unemployment-to-Employment Flows	14
A10	Cyclicality of UE Flows in the OECD	15
A11	Role of EE for the Countercyclicality of New Hires	17
A12	Model Robustness to Including EE hires	19
A13	Voluntary and Involuntary Separations by EE and EUE	20
A14	IRF of Unemployment Rate to a Separation Rate Shock: Data and Models	21
A15	IRF of Labor Productivity to a Separation Rate Shock: Data and Models	21
A16	Separation Shocks: Baseline and Adjusted for Identified Shocks	25
A17	Relative Worker Productivities in the Congestion Model	29
A18	Impulse Responses to a Separation Shock: No-Congestion, Low-Surplus Model	31
A19	Volatility of unemployment, slope of the Beveridge curve and model fit vs K	33
A20	Separation Rate: Measured and Implied	40
A21	Impulse Responses to a Separation Shock: Baseline and Alternative Calibration of Separation Rate Process to Match EU Flows	41
A22	Iso-congestion Curves	45
A23	Impulse Responses to a Separation Shock: Convex Hiring Cost Model	47
A24	Time Paths of Labor Market Variables	49
A25	Unemployment Components	50

A Empirical Appendix: Construction of Worker Flows and Transition Probabilities, and Robustness

In Appendix A.1, we elaborate on our construction of worker flows and measurement of transition probabilities. The rest of the sections provide more details for each of the robustness exercises.

We organize our robustness checks by comparing results to the baseline definition of congestive new hires, which we represent as Okun’s laws (the elasticity of new hires’ outcomes with respect to the unemployment rate, both in log deviations) in Figure A1.

Figure A1: The Countercyclicality of Hiring out of Unemployment: Okun’s Laws and Elasticities



Notes: Panel (a) plots log deviations in the share of employed with some unemployment spell in the preceding year against log deviations in the unemployment rate. The time series are HP filtered with a smoothing parameter of 100. Source: CPS March Supplement (ASEC). Panel (b) plots log deviations in UE flows against log deviations in the unemployment rate. The time series are HP filtered with a smoothing parameter of 1,600. Source: CPS monthly files. We also report elasticities (the linear regression coefficients) for both panels.

Below is a summary list of the robustness checks we undertake:

Time Aggregation Adjustment. For consistency with the discrete time model presented in the main text, the empirical transition rates are not adjusted for time-aggregation bias. In other words, initially employed workers may separate into unemployment and transition back into employment within the period—as in the CPS ASEC definition of asking the end-of-period employed about potential unemployment spells during the period. In Appendix A.2, we find very similar results for the cyclical behavior of these UE flows adjusted for such time aggregation.

Unemployment vs. Nonemployment. In Appendix A.3, in Figures A5 to A8, we replicate Figure 1 by considering the nonemployment (comprising the unemployed and out of the labor force) rather than the unemployment history of the employed, and find qualitatively similar cyclical patterns. While the countercyclicality of NE-hire share in employment exhibits a weaker Okun’s law, our model results would remain unaffected, since the model parameterization would simply require us to estimate a stronger degree of congestion in order to match our empirical calibration targets. In a model extension in Appendix J, we consider flows in and out of the labor force.

Alternative Detrending. In our main specification, we use the conventional smoothing parameter for quarterly data of 1,600 when studying worker flows and transition probabilities (see, e.g., Fujita and Ramey, 2009). Shimer (2005, 2012a) instead chooses a smoothing parameter of 10^5 and accordingly attributes more of the time series variation to cyclical fluctuations. In Appendix A.4, we show that our results are robust to this alternative smoothing parameter. Most importantly, the elasticity of UE flows with respect to the unemployment rate stays unchanged (0.348 vs 0.345) as does the employment share of new hires out of unemployment (0.433 vs 0.432).

OECD Evidence. Appendix A.5 draws on cross country panel data (Elsby, Hobijn, and Sahin, 2013a) and shows that countercyclical UE flows are a feature across the OECD; this fact has been documented (but not studied as a source of amplification) by, e.g., Blanchard and Diamond (1990); Burda and Wyplosz (1994); Fujita and Ramey (2009); Elsby, Hobijn, and Sahin (2013a).

A.1 Baseline: Discrete Data

We use the Current Population Survey (CPS) to measure worker flows. The CPS has a rotating-panel design, in which households are surveyed for four consecutive months, then they rotate out for eight months and then are surveyed for another four months, after which they permanently leave the sample. This structure allows us to match at most three-fourths of the sample in one month to the next. In practice, the matching rate is below 75% due to the temporary absence of individuals from their residence or a household moving out of their address. This phenomenon is referred to as *margin error*.

We start with the monthly micro data covering January 1976 to December 2019 (drawing on the IPUMS platform, see Flood et al., 2022). We restrict our sample to civilians age 15 and above. We categorize each individual in each month t into one of three employment states: employed (E), unemployed (U) and out of the labor force (O). We use final person-level weights to calculate the stock of employed, unemployed and non-participants, $E(t)$, $U(t)$, $O(t)$, for each month t .

Using individual identifiers—using the CPS samples provided by IPUMS and its unique individual ID, CPSIDP, which uses rotation groups, household identifiers, individual line numbers, race, sex, and age to identify individuals—, we calculate individual-level transition events between consecutive months. We again use the current month person-level weights to calculate the total count of worker flows. Let $Z_{ij}(t)$ denote worker flows: the mass of workers in employment state i in month $t - 1$ that are observed in employment state j in month t for $i, j \in \{E, U, O\}$.

To correct for margin error, we make the common *missing at random* (MAR) assumption, which omits missing observations and reweights the measured flows. We adjust our time series by reweighting the measured flows $Z_{ij}(t)$ for $i, j \in \{E, U, O\}$ as follows:

$$\mu_{ij}(t) = \frac{E(t) + U(t) + O(t)}{\sum_i \sum_j Z_{ij}(t)} Z_{ij}(t).$$

The numerator is the worker population implied by measured stocks and the denominator is the population implied by total measured flows, including workers whose employment states do not change. In practice, we construct $\mu_{ij}(t)$ for males and females separately, and then sum them to arrive at our aggregate measure of worker flows adjusted for margin error.

For a number of months in the CPS, it is impossible to match individuals over time. The raw flow series also exhibit several extreme jumps. To deal with missing values and outliers, we follow the approach outlined in Fujita and Ramey (2006) and use the procedure called Time Series Regression with ARIMA Noise, Missing Observations and Outliers (TRAMO, Gomez, Maravall,

and Pena, 1999). We let TRAMO detect additive and transitory outliers using a pre-determined t-test critical level set to 4. Finally, we seasonally adjust the time series using the X-ARIMA-12 procedure developed by the US Census Bureau.

Finally, we calculate the discrete-time job finding and separation probabilities as

$$(A1) \quad \begin{aligned} f_t &= \frac{\mu_{UE}(t)}{U(t-1)} \\ \delta_t &= \frac{\mu_{EU}(t)}{E(t-1)}, \end{aligned}$$

which simply capture the share of unemployed (employed) workers in month $t-1$ who are observed to be employed (unemployed) in month t .

To sum up, the figures we present and our calibration targets in the model are based on our margin-error adjusted flow time series (under the MAR assumption) $\mu_{ij}(t)$, whose missing values and outliers are corrected by the TRAMO procedure, and are seasonally adjusted using the X-ARIMA-12 procedure.

A.2 Robustness: Time-Aggregation-Adjusted Data

Our preferred measure of worker flows is based on discrete time and hence is subject to a specific form of time aggregation bias: drawing on the CPS panel structure, we obtain worker flows by following initially unemployed workers that move into employment by the end of the period (are employed the beginning of next period). One type of transition we miss in this discrete-time approach is that initially employed workers may separate within the period and find a job again, akin to the issues laid out in Shimer (2005).

In this section, we compare the properties of UE flows based on our measurement approach in the main text to a one accounting for time-aggregation bias. Our object of interest is the total number of UE flows within the period, into jobs that remain active until the end of the period, mirroring our definition using the CPS ASEC in Section 1. We also confirm that our time series replicate those reported by Shimer (2012a).

Our Method. We draw on Fujita and Ramey (2006), who provide expressions for time-aggregation-adjusted gross worker flows, whereas our interest is in within-period cumulative UE flows that remain active through the end of the period.

First, we start with the monthly job finding f_t and separation δ_t probabilities, whose measurement are described in Appendix A.1, underlying the analysis in the main text.

Second, we compute the monthly job finding and separation hazards, \widehat{f}_t and $\widehat{\delta}_t$, solving the following system of equations:

$$(A2) \quad \begin{aligned} \delta_t &= u_{ss,t}(1 - e^{-\widehat{f}_t - \widehat{\delta}_t}) \\ f_t &= (1 - u_{ss,t})(1 - e^{-\widehat{f}_t - \widehat{\delta}_t}), \end{aligned}$$

where $u_{ss,t} = \widehat{\delta}_t / (\widehat{\delta}_t + \widehat{f}_t)$ is the steady-state approximation to the unemployment rate implied by the contemporaneous hazard rates. The unemployment law of motion in continuous time is

$$(A3) \quad U_{t-1+\tau} = \frac{(1 - e^{-(\widehat{f}_t + \widehat{\delta}_t)\tau})\widehat{\delta}_t}{\widehat{f}_t + \widehat{\delta}_t} L_{t-1} + e^{-(\widehat{f}_t + \widehat{\delta}_t)\tau} U_{t-1},$$

Table A1: Discrete vs. Time-Aggregation Adjusted Worker Transitions

UE flows	Discrete	Time-aggregation adjusted
Standard deviation	0.045	0.040
Autocorrelation	0.671	0.574
Correlation Matrix		
Discrete	1	
Time-aggregation adjusted	0.983	1

Notes: The table compares the time series properties of UE flows based on our discrete time measurement approach used in the main text to a version corrected for time-aggregation bias. All variables have been logged and the empirical cyclical components have been extracted using the HP-filter with a smoothing parameter of 1,600.

for $\tau \in [0, 1)$ and where L_t is the size of the labor force in month t .

Third, we calculate the number of employed workers at the end of month t who had any unemployment spell during t —which we then compare to the discrete-time-based UE flows. As an intermediate step, we consider the probability of not losing a job, from $t - 1 + \tau$ until t for $\tau \in [0, 1)$, conditional on having a job at t .¹ This probability is given by

$$(A4) \quad \lim_{\Delta \rightarrow 0} \left(1 - \Delta \widehat{\delta}_t\right)^{\frac{1-\tau}{\Delta}} = e^{-\widehat{\delta}_t(1-\tau)}.$$

Using this intermediate result, UE flows during month t , adjusted for time aggregation in that they also count within-period EUE transitions, are given by

$$(A5) \quad UE_t = \int_0^1 \underbrace{\widehat{f}_t}_{\text{Find job}} \underbrace{U_{t-1+\tau}}_{\text{Number of unemployed}} \underbrace{e^{-\widehat{\delta}_t(1-\tau)}}_{\text{Do not lose job}} d\tau.$$

Finally, using Equation (A3), we can integrate out the above expression to obtain UE flows adjusted for time aggregation bias:

$$(A6) \quad UE_t = \widehat{f}_t L_{t-1} e^{-\widehat{\delta}_t} \left(u_{ss,t} \frac{e^{\widehat{\delta}_t} - 1}{\widehat{\delta}_t} + \left(\frac{U_{t-1}}{L_{t-1}} - u_{ss,t} \right) \frac{1 - e^{-\widehat{f}_t}}{\widehat{f}_t} \right).$$

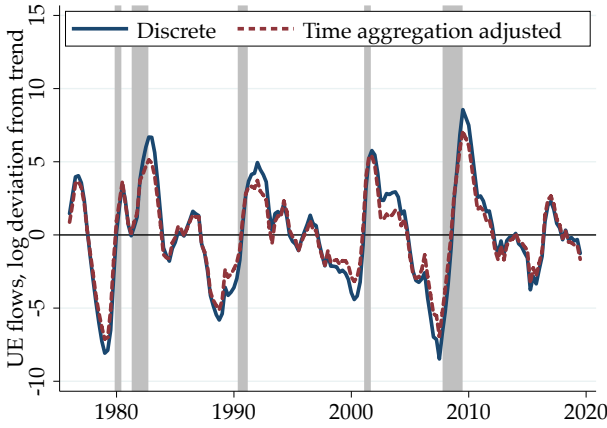
Table A1 summarizes the properties of the discrete-time and time-aggregation-adjusted series. The two time series have extremely similar standard deviations and autocorrelations, and are nearly perfectly correlated.

Figure A2 Panel (a) reports the time series of UE flows in our baseline definition based on discrete time measurement, along with the time-aggregation-adjusted time series. Panel (b) shows the Okun’s law, such that the elasticity of UE flows adjusted for time aggregation bias with respect to the unemployment rate is 0.265, similar to the elasticity arising from the discrete-time approach in Figure A1 Panel (b), where we estimated an only slightly higher elasticity of 0.345. Hence, our congestion dynamics are robust to time-aggregation adjustment, i.e., to counting within-period EUE flows in addition to the transitions into employment for the initially unemployed.

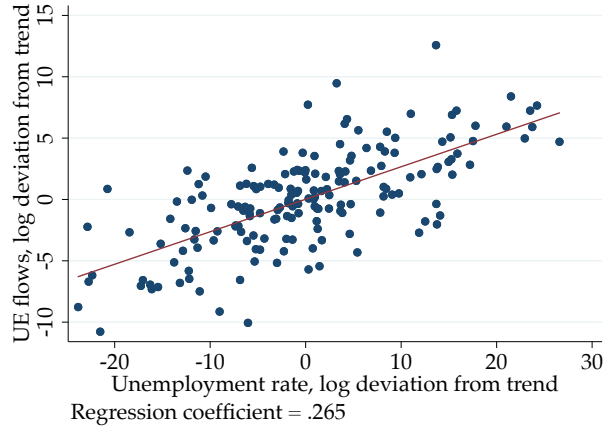
¹Therefore, our results do not study cycles such as “E(UEUEU)E” transitions during the period. These are comparatively tiny compared to the first-order flows stemming from the initially employed losing their job during the period, becoming reemployed, and not losing that first-found job again.

Figure A2: Comparing Discrete and Time Aggregation Adjusted UE Flows

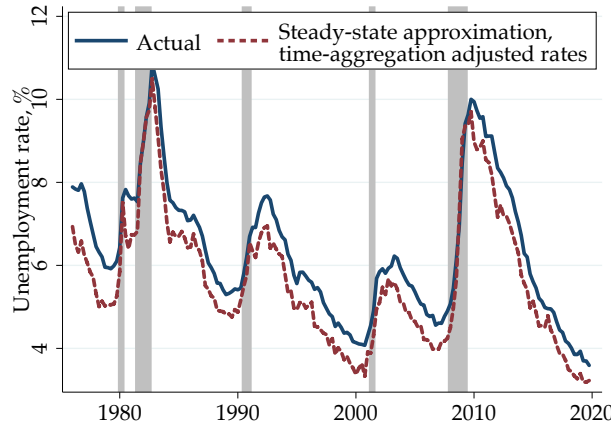
(a) UE Flows: Discrete vs. Time Aggregation Adjusted



(b) UE Flows vs. Unemployment Rate



(c) Unemployment Rate



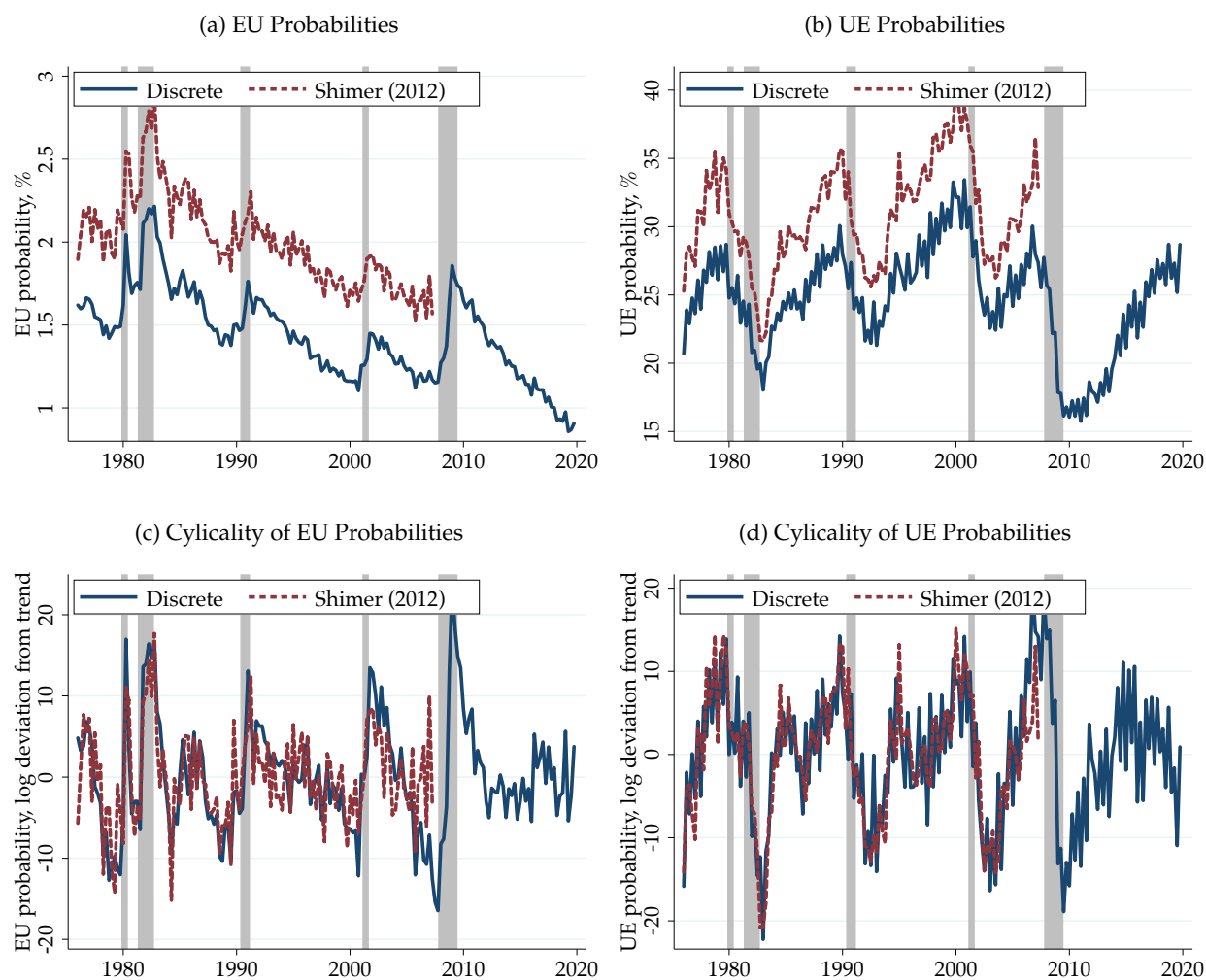
Notes: The figure shows robustness of the UE flows to time aggregation bias adjustment. Panel (a) reports the time series of UE flows in our baseline definition based on discrete time, along with the time-aggregation-debiased time series. Panel (b) is a scatter plot of UE flows adjusted for time aggregation bias against the unemployment rate. Panel (c) plots the actual unemployment rate and its steady-state approximation based on time-aggregation adjusted hazard rates, \hat{f} and $\hat{\delta}$. All time series are based on quarterly averages of monthly data and are logged and HP-filtered using a smoothing parameter of 1,600. Source: CPS monthly files.

To gauge the accuracy of the time-aggregation adjusted hazard rates, \hat{f} and $\hat{\delta}$, in Panel (c) of Figure A2, we further plot the actual unemployment rate as well as its steady-state approximation $u_{ss,t}$. The steady-state approximation tracks the actual time series closely, lending credibility on the measurement exercise in this section.

Comparison to Shimer (2012a). To further highlight the robustness and validity of our empirical analysis, we compare our preferred worker transition probabilities to the ones reported in Shimer (2012a).² Panel (a) in Figure A3 plots the employment-to-unemployment probability used in the

²This data was constructed by Robert Shimer. For additional details, please see Shimer (2012a).

Figure A3: Comparing Discrete and Time Aggregation Adjusted Flow Probabilities



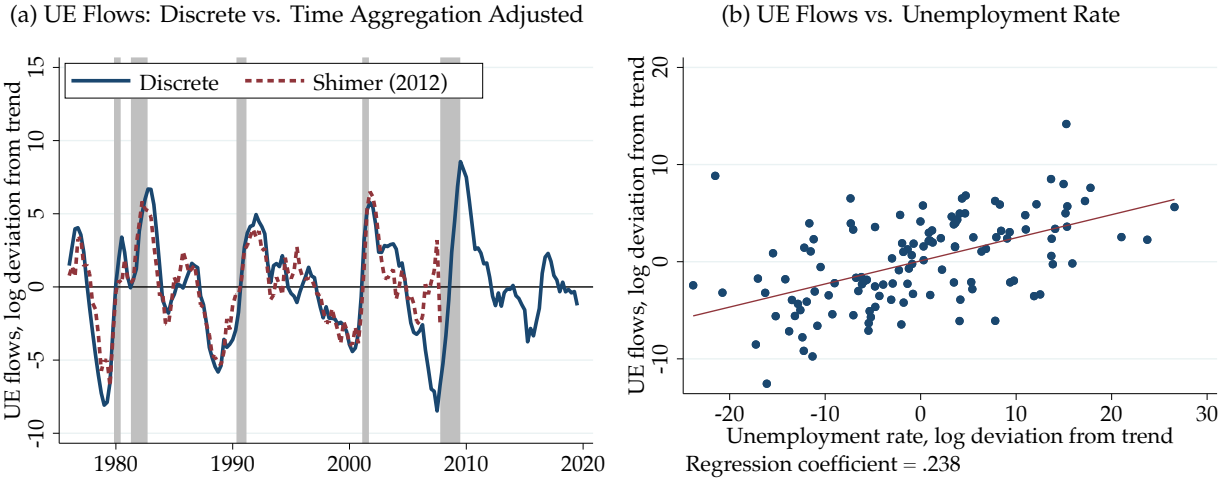
Notes: Panel (a) compares the EU probability used in the main text to its time-aggregation adjusted counterpart provided by Shimer (2012a) allowing for flows between employment, unemployment and inactivity. Panel (b) does the same for UE probability. Panels (c) and (d) plot the log deviations of these probabilities from their respective trends. The series are logged and HP-filtered using a smoothing parameter of 1,600. Source: CPS monthly files.

main text and compares that to the same monthly probability adjusted for time aggregation bias provided by Shimer (2012a). Panel (b) does the same for unemployment-to-employment flows. While the time-aggregation adjusted probabilities are higher in levels, their cyclical behavior closely tracks the underlying discrete-time probabilities that we use in our main analysis (Panels (c) and (d)).

While Shimer (2012a) does not report the properties of UE flows in the paper, the similarity of the cyclical behavior of the transition rates also implies that the UE flows implied by the Shimer (2012a) data would be similarly countercyclical.³ For comparison with our main analysis, we

³Shimer (2012a) does not present UE flows, but focuses on transition rates. In the discussion of the prior evidence, he writes: “In fact, even after accounting for time aggregation, the decline in the job finding probability almost exactly offsets the increase in the number of unemployed workers at business cycle frequencies, so the number of unemployed

Figure A4: Comparing Discrete and Time Aggregation Adjusted UE Flows (Shimer 2012)



Notes: The figure shows robustness of the UE flows to time aggregation bias adjustment allowing for worker flows between three labor market states. Panel (a) reports the time series of UE flows in our baseline definition based on discrete time, along with the time-aggregation-debiased time series. Panel (b) is a scatter plot of UE flows adjusted for time aggregation bias against the unemployment rate. All time series are based on quarterly averages of monthly data and are logged and HP-filtered using a smoothing parameter of 1,600. Source: CPS monthly files.

calculate the time-aggregation-adjusted UE flows simply as

$$(A7) \quad UE_t^{\text{Shimer}} = U_{t-1} \Lambda_{ue,t},$$

where $\Lambda_{ue,t}$ is the monthly probability of a UE flow provided by Shimer (2012a).

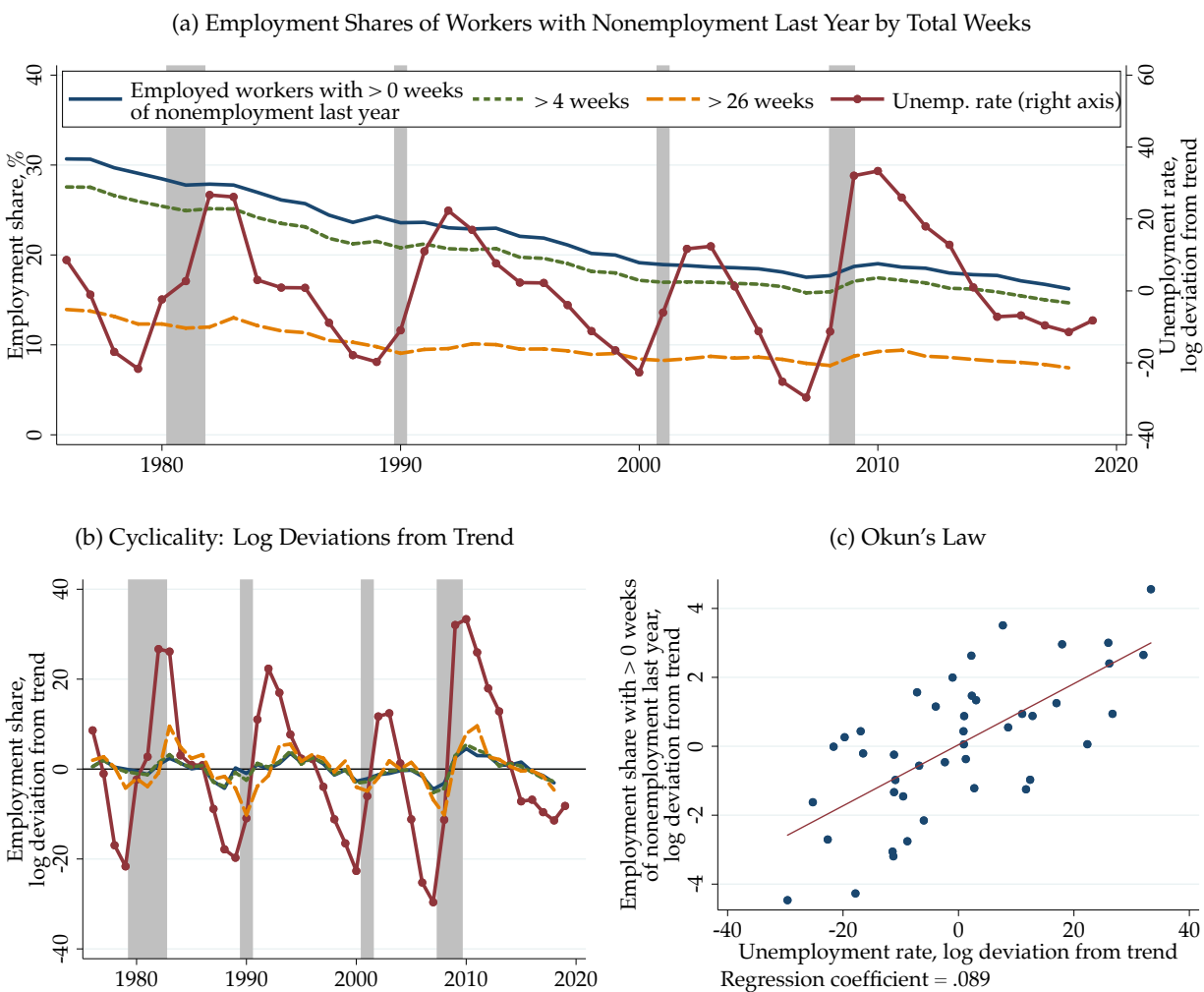
Figure A4 compares our baseline measure of UE flows to the one based on Shimer (2012a). Panel (a) plots the cyclical component of UE flows over time and shows that UE flows adjusted for time aggregation in a three-state model also exhibit strong countercyclicality. Panel (b) quantifies this countercyclicality: the elasticity of UE flows with respect to the unemployment rate is 0.257, slightly lower than the elasticity we report in the main text.

A.3 Robustness to Nonemployment rather than Unemployment, i.e., Including Previous Non-participants in New Hires

Below in Figures A5 to A8, we provide similar figures to those presented in the main text by including workers who flow into employment from non-participation. In Figure A5, we replicate Figure 1 by considering the nonemployment (comprising unemployment and out of the labor force) rather than the unemployment history of the employed, and find qualitatively similar cyclical patterns. While the countercyclicality of NE-hire share in employment exhibits a weaker Okun's law, our model results would remain unaffected, since the model parameterization would simply require us to estimate a stronger degree of congestion (lower σ) in order to match our empirical calibration targets.

workers who find a job in a month shows little cyclicity" (page 145). Our reading is that this statement likely assesses the amplitude of log UE flows (i.e., percent deviations from trend) when compared with the amplitude of percent deviations from trend of the transition rates and probabilities, rather than a different conclusion of the qualitative nature about the countercyclicality of UE flows.

Figure A5: Countercyclicity of the Employment Share with Nonemployment Past Year



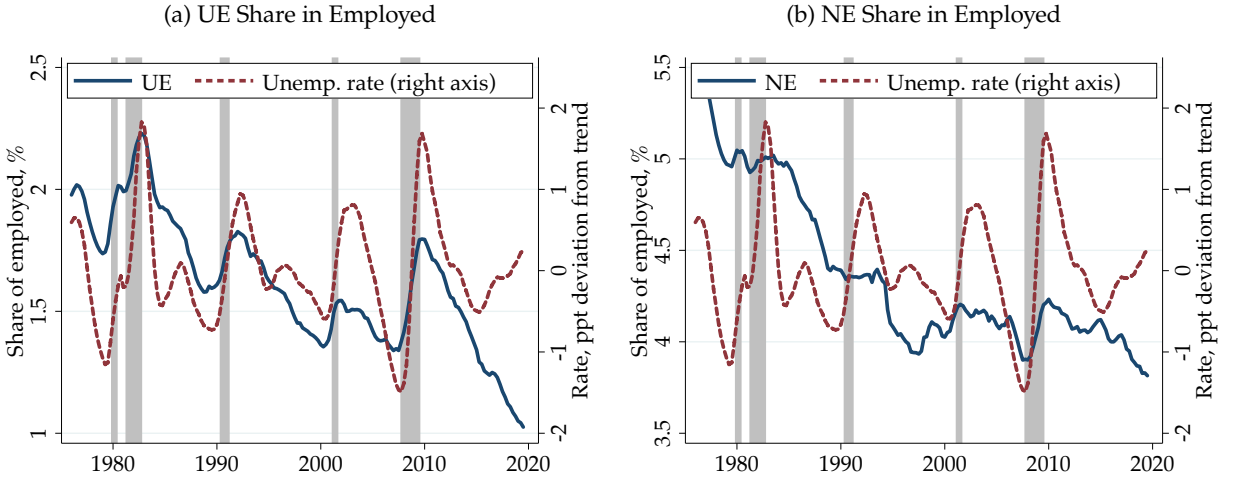
Notes: The figure replicates Figure 1, but instead conditions on *nonemployment* duration, i.e., we also include labor market states where a worker might be out of the labor force. Panel (a) plots the share of employed workers who have undergone a nonemployment spell in the preceding calendar year for different nonemployment durations. Panel (b) plots their log deviations from trend. Panel (c) reports the scatter plot of the detrended time series. The time series are HP filtered with a smoothing parameter of 100. Shaded regions denote NBER-dated recessions. Source: CPS March Supplement (ASEC).

A.4 Alternative HP Smoothing Parameter

In the main text, we report business cycle statistics based on HP-filtered time series with a smoothing parameter of 1,600, typically used for quarterly data. In this section, we instead use a smoothing parameter of 10^5 —preferred by Shimer (2005, 2012a)—to report business-cycle statistics.

Table A2 reports the standard deviations, auto- and cross-correlations of the HP-filtered time series we present in the main text. With a smoothing parameter more aggressively penalizing movements in the trend components in the time series, the standard deviations of the variables around these trends become considerably higher. The cross-correlations between f , δ and UE/E

Figure A6: The Countercyclicity of New Hire Share: CPS Worker Flows



Notes: Panel (a) plots the share of UE hires in employment. Panel (b) plots NE flows in the share of employed. All time series are based on quarterly averages of monthly data and for visual clarity are smoothed by taking centered four-quarter moving averages. Both panels also plot the percentage point deviation of unemployment rate from its trend on a secondary axis. Shaded regions denote NBER-dated recessions. Source: CPS monthly files.

become if anything even more pronounced.⁴

Table A2: Business Cycle Properties: Alternative Smoothing Parameter

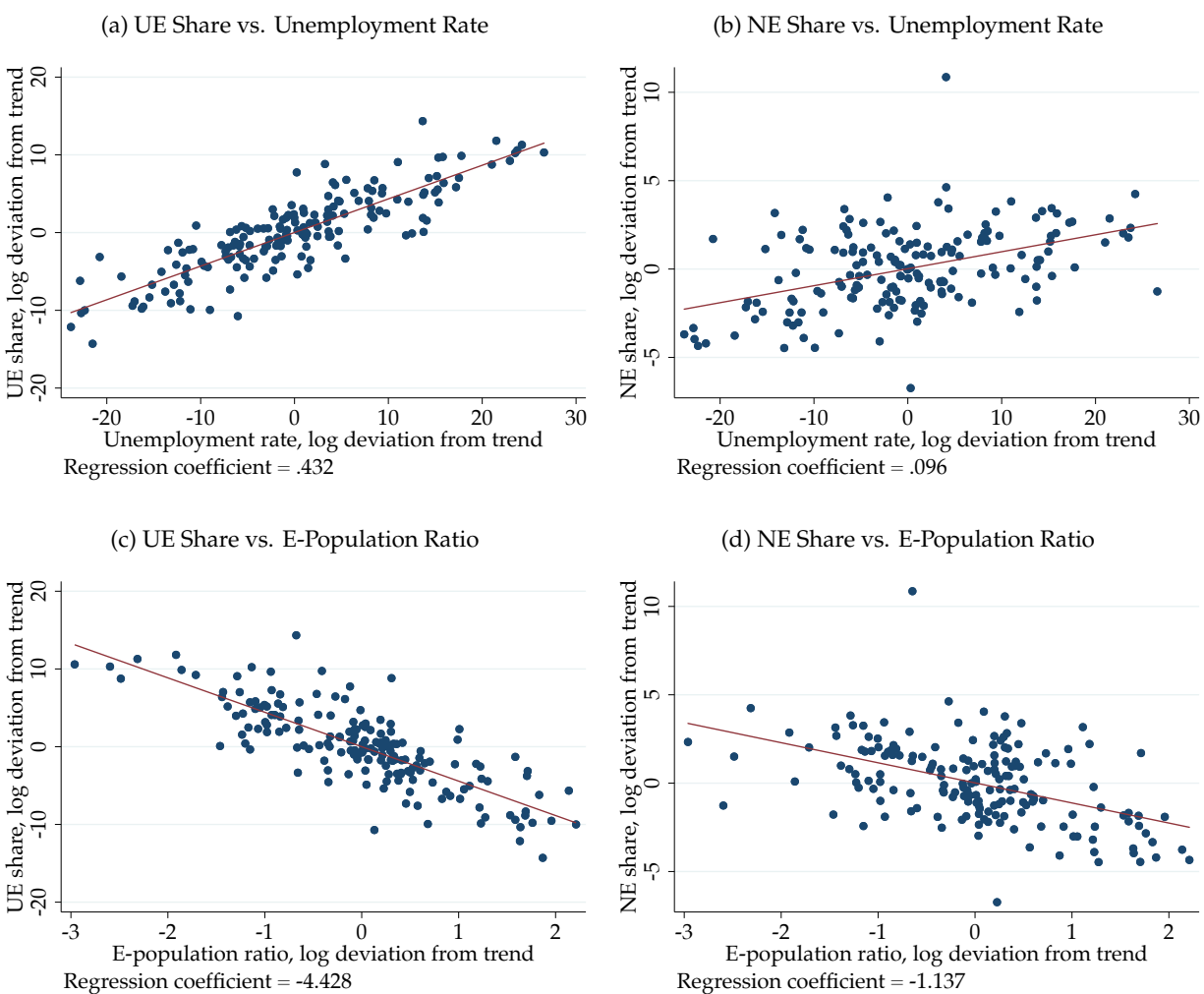
	ALP	f	δ	u	v	θ	UE/E
Standard deviation	0.017	0.093	0.108	0.190	0.198	0.376	0.116
Autocorrelation	0.897	0.950	0.904	0.970	0.957	0.962	0.933
Correlation matrix							
ALP	1						
f	-0.061	1					
δ	-0.179	-0.860	1				
u	0.015	-0.975	0.919	1			
v	0.050	0.831	-0.831	-0.851	1		
θ	0.038	0.906	-0.877	-0.928	0.978	1	
UE/E	0.113	-0.888	0.783	0.930	-0.718	-0.818	1

Notes: ALP , f , δ , u , θ and UE/E indicate, respectively, average labor productivity, the job finding rate, separation rate, unemployment rate, labor market tightness and share of new hires in employment. All variables have been logged and the empirical cyclical components have been extracted using the HP-filter with the alternative smoothing parameter of 10^5 rather than 1,600.

Most importantly, Figure A9 presents scatter plots of UE flows and shares against the unemployment rate, respectively, under this alternative smoothing parameter. The elasticity of UE flows

⁴The correlation of average labor productivity with the job finding rate (unemployment rate) turns slightly negative (positive), likely due to the inclusion of additional years compared to Shimer (2005), and consistent with our aforementioned comment that ALP is not an obvious cyclical driver (see, e.g., Shimer, 2005; Mitman and Rabinovich, 2020; Gali and Van Rens, forthcoming).

Figure A7: Cyclicity of Share of New Hires in Employment: CPS Worker Flows



Notes: The figure plots different measures of new-hire share in employment (UE or NE) against employment measures (unemployment rate or employment-population ratio). All time series are based on quarterly averages of monthly data and are logged and HP-filtered using a smoothing parameter of 1,600. Source: CPS monthly files.

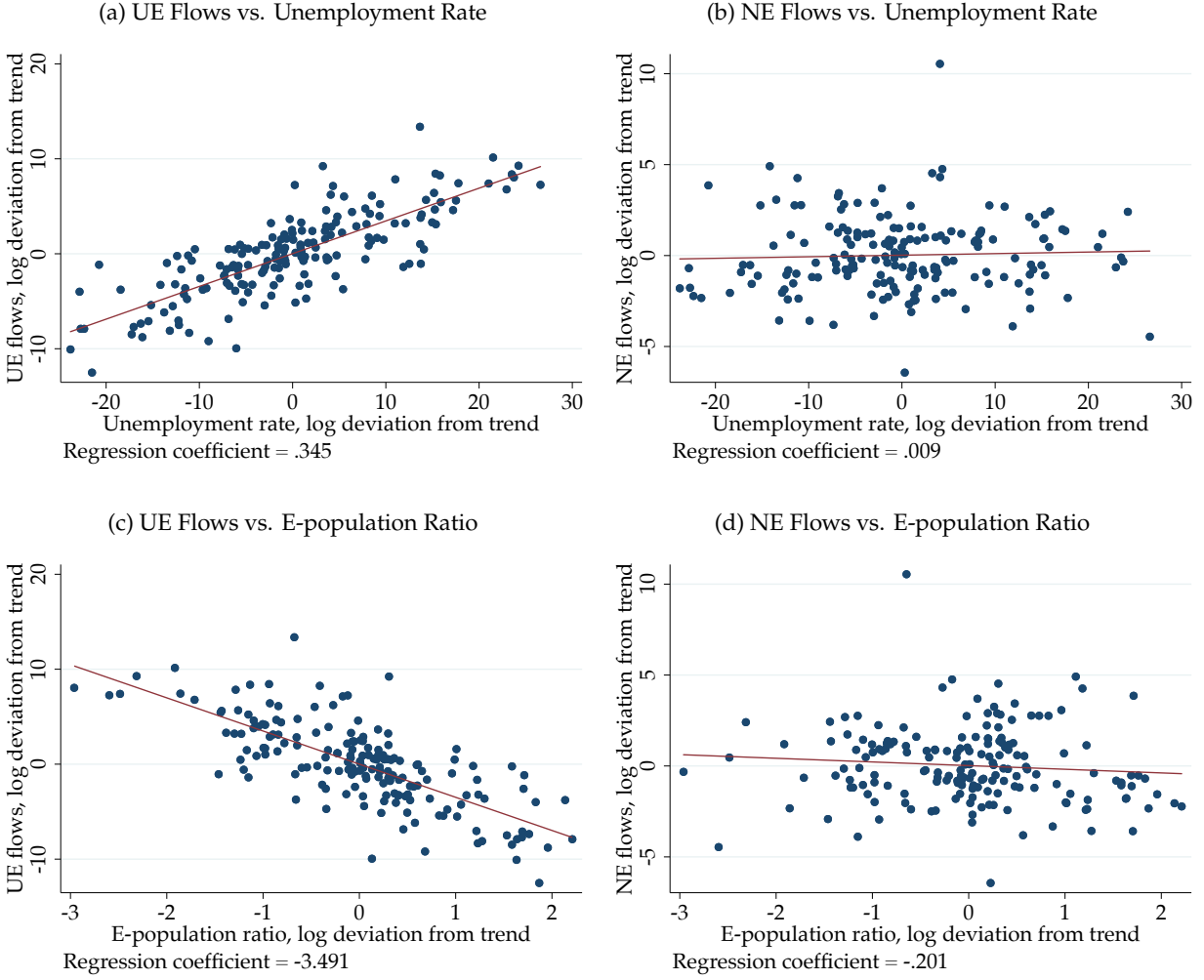
with respect to the unemployment rate is almost identical to the one we present in Figure A1 Panel (b) (0.348 vs 0.345). Likewise, the elasticity of new-hire share in employment to the unemployment rate stays unchanged compared to the one reported in Figure A7 Panel (a) (0.433 vs 0.432).

We conclude that our key facts are robust to an alternative smoothing parameter of 10^5 preferred by Shimer (2005, 2012a).

A.5 Evidence from OECD Countries

The countercyclicity of UE flows extends to many OECD countries. In Figure A10 Panel (a), we plot the elasticity of UE flows with respect to the unemployment rate for a set of OECD countries, drawing on transition rates estimated in Elsby, Hobijn, and Sahin (2013a) on the basis of labor force survey data and unemployment stocks.

Figure A8: Cyclicity of New Hires: CPS Worker Flows



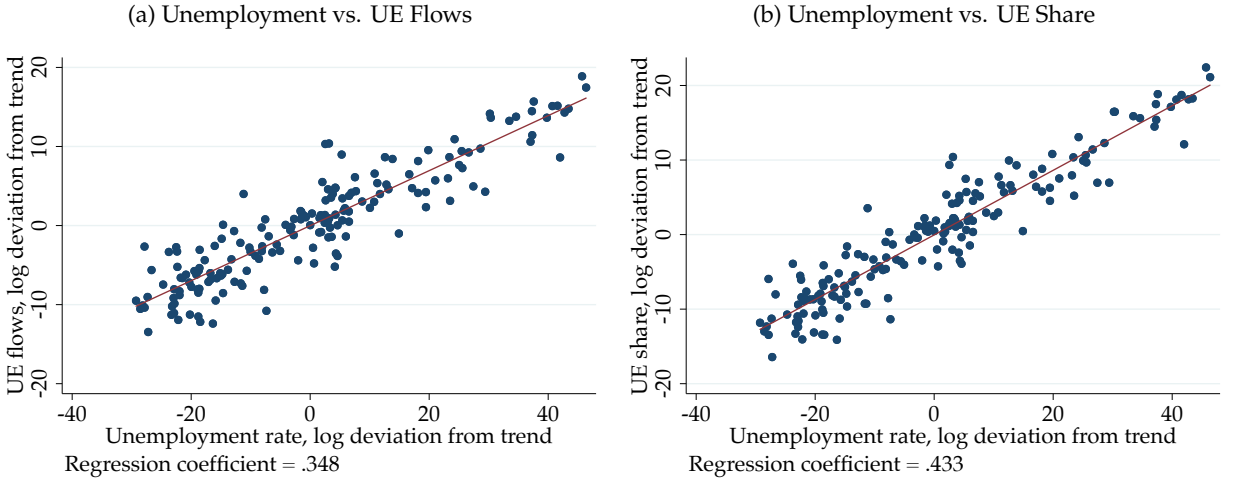
Notes: This figure is a complement to Figure A7. The figure plots different measures of new-hire flows into employment (UE or NE) against employment measures (unemployment rate or employment-population ratio). All time series are based on quarterly averages of monthly data and are logged and HP-filtered using a smoothing parameter of 1,600. While our model relies on the share of new hires in employment rather than worker flows, this figure presents the cyclical behavior of nonemployment-to-employment flows, which are nearly acyclical, but importantly remain countercyclical as a share of (procyclical) employment, in turn presented in Figure A5. Source: CPS monthly files.

As a validation check, we point out another perspective on the elasticity of UE flows with respect to the unemployment rate, repeated below for convenience

$$(A8) \quad \varepsilon_{UE,u} = \frac{df/f}{du/u} + 1 = \left((1-u) \left[-1 + \frac{d\delta/\delta}{df/f} \right] \right)^{-1} + 1.$$

Building on the insight that the unemployment rate fluctuations implied by the job finding rate shift only is $du^f/u^f = -(1-u)df/f$. Fujita and Ramey (2009) show that the regression coefficient of du^f/u^f on du/u also represents the share of the variance in unemployment rate fluctuations due to fluctuations in the job finding rate (rather than in the job separation rate). The smaller this

Figure A9: The Countercyclicity of Unemployment-to-Employment Flows

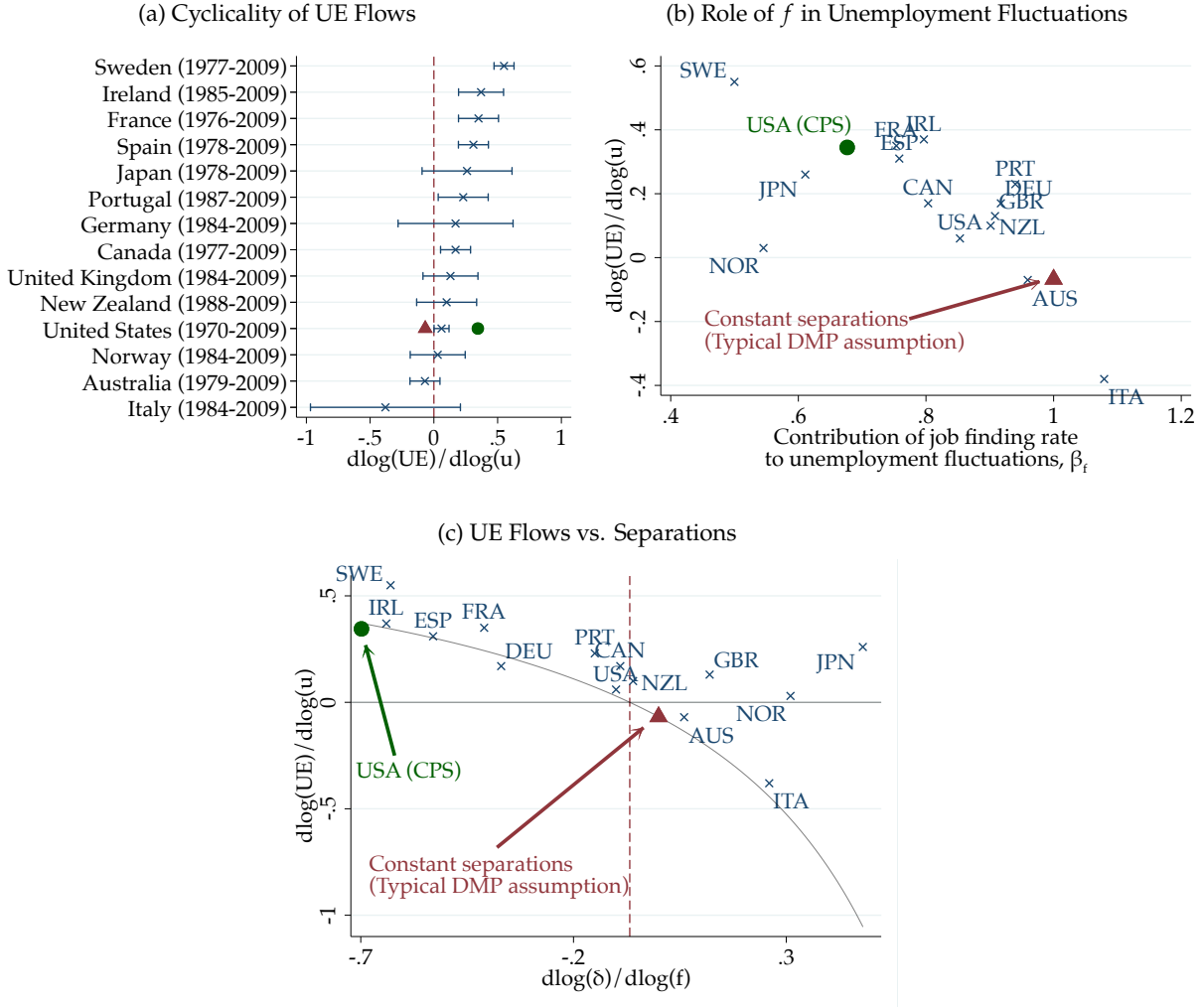


Notes: Panel (a) plots the log deviations in UE flows and log deviations in the unemployment rate from their respective trends. Panel (b) plots log deviations in UE share in employment against log deviations in the unemployment rate. All series are based on quarterly averages of monthly data. Detrended series are HP filtered with a smoothing parameter of 10^5 . Source: CPS monthly files.

share, the more countercyclical the UE flows on average, since $\frac{dUE/UE}{du/u} = -\frac{1}{1-u} \frac{du^f/uf}{du/u} + 1$. Drawing on cross-country differences in the OECD, we document the empirical validity of this theoretical property in Panel (b) of Figure A10, a scatterplot that shows a clear negative relationship between the elasticity against the contribution of job finding rate to unemployment fluctuations, the latter computed in Elsby, Hobijn, and Sahin (2013a). Since we apply steady-state approximations while Elsby, Hobijn, and Sahin (2013a) point out that in many OECD countries dynamic expressions are appropriate, and since the unemployment rates are not homogeneous, this scatter plot does not trace out a perfectly straight line.

Finally, Panel (c) plots the UE flows-unemployment rate elasticity against the job finding-job separation rate elasticity in our sample of OECD countries, together with the theoretical relationship between the two as determined by Equation (A8). Broadly, the relationship between the two elasticities holds across countries (with the approximation error reflecting the assumptions of stationarity and having only two labor market states).

Figure A10: Cyclicity of UE Flows in the OECD



Notes: Panel (a) plots the elasticity of UE flows with respect to the unemployment rate in a set of OECD countries. Panel (b) plots these elasticities against the importance of job finding rate fluctuations in explaining the volatility in unemployment for each country. To compute the contribution of the job finding rate to unemployment fluctuations based on monthly CPS data (green dot), we calculate $\text{cov}(-(1 - \bar{u}_{ss})\hat{f}, u_{ss})/\text{var}(u_{ss})$, where u_{ss} is the steady-state approximation to the unemployment rate, \bar{u}_{ss} is its trend and \hat{f} is the cyclical component of (log) job finding rate (see Fujita and Ramey, 2009), such that $-(1 - \bar{u}_{ss})\hat{f}$ is the unemployment rate deviation due to the job finding rate only. For the DMP model without separation shocks, this share is one, and the elasticity on the y-axis is computed using formula (A8). Panel (c) plots the elasticity of UE flows with respect to the unemployment rate as well as the theoretical relationship between the two based on a steady state approximation. Source: Elsby, Hobbijn, and Sahin (2013a) and CPS monthly files.

B Robustness: Job-to-Job Transitions and Total Hires

Our model studies countercyclical congestion in jobs filled by workers hired out of unemployment, their share in employment, and (their effect on) flows between unemployment and employment. In our model, we ignore job-to-job transitions, because we view those hires as filling different types of jobs. For instance, Faberman et al. (2022) use novel survey data and show that outcomes from job search greatly differ for the employed compared to the non-employed, leading to higher wages and better jobs. This happens despite EE search itself being more pervasive at the “lower rungs” of a job ladder. *Ultimately, our paper however does not resolve this open question, but explores the consequences of treating UE hires as different than EE hires.*

As noted in the main text, while UE flows are countercyclical, job-to-job transitions (and quits) drop dramatically in recessions (see, e.g., Mercan and Schoefer, 2020). In fact, total hires—rather than those only out of unemployment—are not countercyclical. In this appendix, we assess robustness of our congestion mechanism to relaxing the assumption that EE hires do not cause congestion.

Empirical Behavior of a Broader Notion of Congestive Hires that Includes EE Switchers. We consider the implications of a broader notion of congestive hires that include a (constant) share $a \in [0, 1]$ of EE hires:

$$(A9) \quad \tilde{H}_t = a \cdot EE_t + UE_t,$$

where we continue to assume that all UE flows are congestive as in our baseline measure.

We start our analysis by describing the empirical behavior of this broader notion of congestive hires in the US data, for various values of a . To construct EE hires, we multiply the EE rate (computed by Fujita, Moscarini, and Postel-Vinay (2020a) using the CPS) by the employment mass.⁵ Since EE transitions can only be measured starting in 1995 in the CPS, we restrict this analysis to 1995–2019.

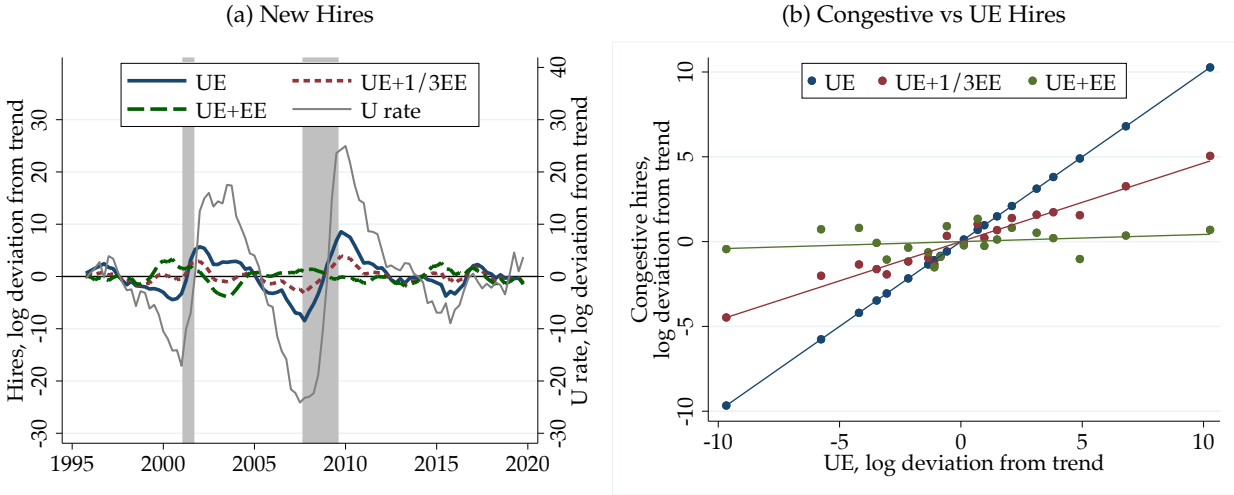
Figure A11 Panel (a) clarifies the role of EE hires in determining the cyclicity of congestive new hires. The case of $a = 0$ (solid blue line), where EE hires are not considered congestive, is our baseline measure in which congestive hires are strongly countercyclical. As we assume a larger share a , this countercyclicity is dampened. Panel (b) is a scatterplot that illustrates the comovement of total congestive hires and UE hires (both in log deviations from trend), for three values of $a \in \{0, 0.1/3, 1\}$. Panel (c) traces out the elasticity of congestive hires with respect to UE hires for the full range of $a \in [0, 1]$.

Consider the extreme case of $a = 1$ (green lines in Panels (a) and (b)), where all EE flows are considered congestive. This concept of new hires corresponds to “total hires” simply counting all new job starts from unemployment and employment. In this case, total hires do not actually increase with UE flows.⁶ In sum, a higher share of (procyclical) EE flows that is assumed congestive counteracts (countercyclical) UE flows.

⁵We treat EE and UE flows consistently in our empirical analysis, using the same timing conventions as described in Appendix A.1. In particular, we multiply the EE rate between $t - 1$ and t with the mass of employment in period $t - 1$ to calculate the mass of EE flows between $t - 1$ and t . We prefer to use the measure provided by Fujita, Moscarini, and Postel-Vinay (2020a), which corrects for the sharp increases in the incidence of missing answers to the relevant CPS question identifying EE transitions starting in 2007 due a change in the survey design, which would significantly bias the measured post-2007 EE rate downwards and change its cyclical properties.

⁶We have alternatively also computed the elasticity of total hires to the unemployment rate; for values of a above 0.6, the total hires measure becomes even positively correlated with the unemployment rate; our preferred values of a explored here are below that cutoff and hence preserve the countercyclicity of the congestive hires measure.

Figure A11: Role of EE for the Countercyclicity of New Hires



(c) Sensitivity of Congestive Hires to EE Hires

Notes: Panel (a) plots the log deviations in quarterly averaged monthly hires for different measures of “congestive” EE hires (shares 0, 1/3 and 1) over time. The unemployment rate is included as a business-cycle indicator. The time series are smoothed by taking centered four-quarter moving averages for visual clarity. Panel (b) scatter plots congestive hires against UE hires for different measures of congestive EE hires (shares 0, 1/3 and 1). Panel (c) plots the elasticity of congestive hires with respect to UE hires as a function of the share of EE hires that is assumed to be congestive. The vertical line marks our preferred share of $a = 1/3$. All time series are HP filtered with a smoothing parameter of 1,600. Source: CPS and Fujita, Moscarini, and Postel-Vinay (2020a).

Quantitative Assessment in the Model. We now turn to a quantitative treatment of procyclical EE hires. Namely, we introduce a simple, albeit ad-hoc, notion of congestive EE hires into our model which is meant to mimic job-to-job transitions in the absence of formally modelling on-the-job search. Next, we show robustness of our quantitative results to the attenuation brought about by procyclical EE hires. As our model does not feature on-the-job search and in order to preserve comparability of the augmented model to our baseline while retaining the calibration targets, we introduce the following *single* change: we assume an imperfect pass-through from UE hires to

congestive hires at $k = 1$, given by:⁷

$$(A10) \quad e_{1,t} = u_{t-1}f_{t-1} \left(\frac{u_{t-1}f_{t-1}}{\bar{u}\bar{f}} \right)^\gamma,$$

where $1 + \gamma \leq 1$ is the elasticity of congestive hires with respect to UE hires, and \bar{u} and \bar{f} denote the steady-state values of the unemployment rate and the job finding rate, respectively. Here, workers with $k = 1$ are the congestive hires and uf is the model counterpart to UE flows.

This model object maps into the empirical definition in Equation (A9) but simplifies it for our purposes to capture the attenuation in the countercyclical behavior of congestive hires brought about by the additional EE hires. It does so by introducing two simplifications. First, this specification avoids increasing the steady-state level of hires to isolate level effects from the cyclical behavior of the hires across different values of a (in order to isolate effects from the cyclical behavior of the hires time series). Second, it only captures movements in non-UE hires that are related to the baseline measure of UE hires. This approach helps us avoid introducing another shock or source of volatility to the model.

In this specification, the attenuation parameter γ is the crucial parameter, pinned down by the elasticity of congestive hires, which is plotted in Figure A11 Panel (c) for each a share of congestive hires among EE flows. When $\gamma = 0$ ($a = 0$) this elasticity is unity and we nest the benchmark model. When $\gamma < 0$ ($a > 0$) however, the countercyclical behavior of congestive hires is dampened, mimicking the effect of including EE hires among congestive hires. For example, $\gamma = -1$ implies that congestive hires become completely insensitive to new hires out of unemployment, akin to assuming all EE flows are similar to UE flows and hence congestive hires are acyclical, rendering our mechanism ineffective. We then study the quantitative performance of our model for a range of γ values, corresponding to a range of a values. Figure A11 Panel (c) plots the empirical correspondence between the elasticity and a , and hence subtracting 1 from the elasticity gives the correspondence between the model object γ and a .⁸

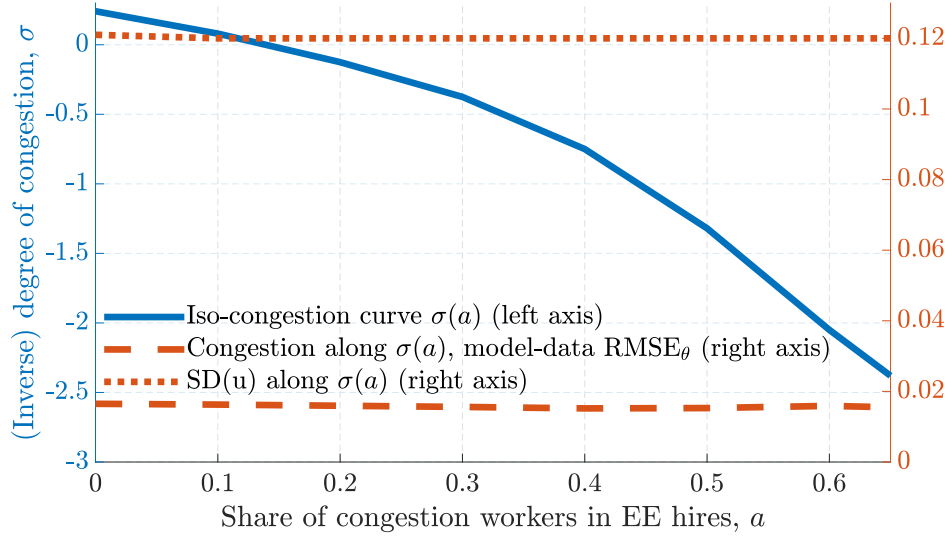
Model Behavior and γ . In Figure A12, we feed the empirical estimates for γ corresponding to each a value and estimate the corresponding congestion parameter σ that minimizes the distance between the model and empirical IRFs of labor market tightness with respect to the separation rate—the same parameterization strategy as in our baseline model.

For concreteness, the x-axis of the figure is in terms of a rather than γ . Similar to our results before, we find that a higher congestive EE share,—less countercyclical congestive hires, including UE and some of EE—requires a more negative congestion parameter σ to match the empirical labor market tightness behavior to separation rate shocks in the model. Once this key parameter is recalibrated to match the target disciplining the degree of congestion, the model again generates the same level of unemployment fluctuations. We conclude that as long as congestive hires remain countercyclical, the model's quantitative performance is preserved up to a recalibration of the key congestion parameter.

⁷To maintain a constant labor force normalized to one, we adjust the remaining mass of employed workers as $e_{k,t} = (1 - \rho_{t-1})e_{k-1,t-1} - \frac{e_{k-1,t-1}}{E_{t-1}-e_{1,t-1}}u_{t-1}f_{t-1} \left(\left(\frac{u_{t-1}f_{t-1}}{\bar{u}\bar{f}} \right)^\gamma - 1 \right)$ for $k \geq 2$.

⁸From Equation (A9), the correspondence between γ and a is approximately given by $\gamma = \varepsilon_{H,UE} - 1 = \frac{aEE}{aEE+UE}(\varepsilon_{EE,UE} - 1)$, where $\varepsilon_{H,UE}$ and $\varepsilon_{EE,UE}$ denote the elasticity of congestive and EE hires with respect to UE hires, respectively. In our sample, we have $\varepsilon_{EE,UE} = -0.565$ and a ratio of average EE hires to average UE hires of $EE/UE = 3.46M/2.01M = 1.72$.

Figure A12: Model Robustness to Including EE hires



Notes: This figure plots recalibrated values of σ for different shares of congestive EE hires, a , the “iso-congestion” curve $\sigma(a)$, by feeding in the corresponding γ from Figure A11 Panel (c). It also plots the RMSE between the empirical and model-implied IRF of labor market tightness to separation shocks, and the standard deviation of unemployment for the recalibrated model to highlight that the congestion and amplification properties of the model stay the same as long as σ is recalibrated to match the market-tightness impulse response target.

Calibrating $a \approx \frac{1}{3}$: Which Share of EE Hires Congests UE Hires? We close with a tentative assessment of a realistic level of a . The suggestive measure we devise for a builds on the Survey of Income and Program Participation (SIPP), accessed from the NBER Public Use Data Archive, which, unlike the CPS, provides separation reasons from a job for both EE switchers and EU separators. We keep record of the reason of separation from last job for UE switchers and denote them by (E)UE. The idea is that this self-reported measure permits us to, imperfectly, strip out the voluntary switches (involving moves up the job ladder across firms that if anything enhance productivity) and isolate transitions that may be similar to the involuntary separations and associated drops to $k = 1$ of unemployed job seekers.⁹

Slightly generalizing our empirical measure of congestive hires above, we permit a share $a^{(E)UE}$ out of unemployment and a share a^{EE} from employment to be congestive. Permitting $a^{(E)UE} < 1$ is important to not understate a . That is, formally, the mass of congestive hires is given by:

$$(A11) \quad \tilde{H}_t = a^{EE} \cdot EE_t + a^{(E)UE} UE_t = a^{(E)UE} \left(\frac{a^{EE}}{a^{(E)UE}} \cdot EE_t + UE_t \right),$$

where the constant $a^{(E)UE}$ drops out when we take logs and detrend the data. Therefore, the share a above would more precisely corresponds to $\tilde{a} = \frac{a^{EE}}{a^{(E)UE}}$.

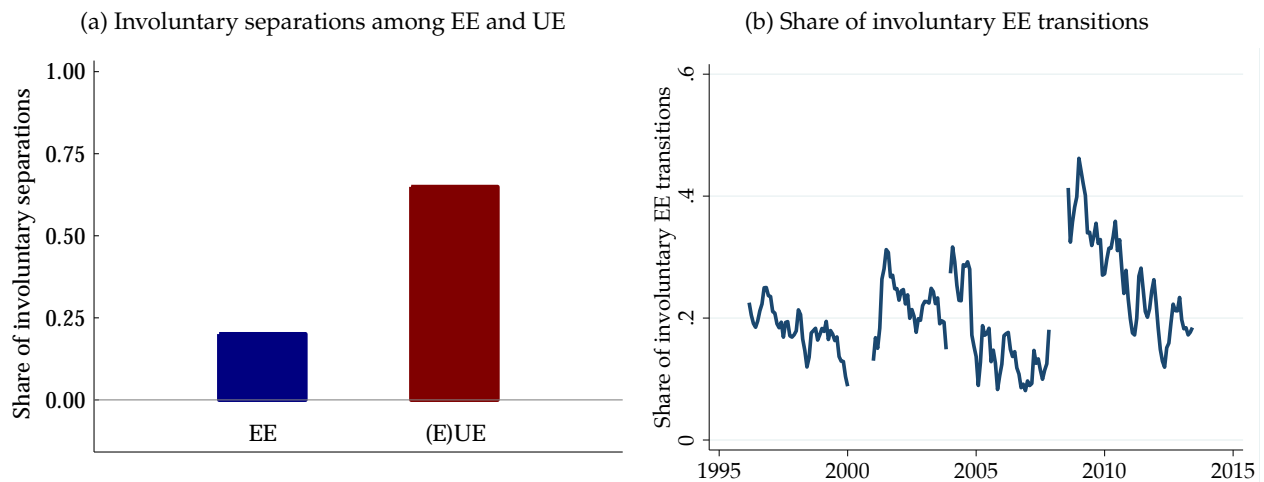
Figure A13 Panel (a) plots the share of involuntary (employer-initiated) EE transitions (sample average 20%) and (E)UE transitions (sample average 65%). These values imply a share \tilde{a} of about one

⁹While constructing this measure of voluntary vs involuntary separations, we follow Nagypál (2008) in categorizing worker separations into two broad groups: i) Voluntary separations comprising personal quits (retirement, child care, other family reason, illness, injury, schooling) and job-related quits (quit to take another job, unsatisfactory work arrangements, other quits), ii) Involuntary separations comprising employer-initiated separations (on layoff, discharged or fired, employer bankrupt, business sold, slack work or business conditions) and end of temporary jobs.

third (20/65). Panel (b) plots the time series of the share of EE hires that are involuntary; that share increases in, e.g., the Great Recession. If anything, involuntary separations increase (as a share of EE transitions, which overall decrease in level) in the Great-Recession. Hence, our simplified assumption of a constant congestive EE share is conservative, attenuating our mechanism.

Our choice for a is also close to related existing estimates. The quantitative exercise in Faberman et al. (2022) implies a “reallocation share” (EE switchers whose outside offer is unemployment rather than their current job) within EE transitions of $1/2.5 = 0.4$. Jolivet, Postel-Vinay, and Robin (2006) use data from the PSID and a structural model targeting the share of EE transitions with wage cuts to estimate that around one third of EE transitions are due to reallocation. Similarly, Tjaden and Wellschmied (2014) document that in the 1993 and 1996 SIPP panels, around one third of EE transitions are associated with nominal wage cuts and using a quantitative search model, they find that 60% of such transitions are due to reallocation shocks.

Figure A13: Voluntary and Involuntary Separations by EE and EUE

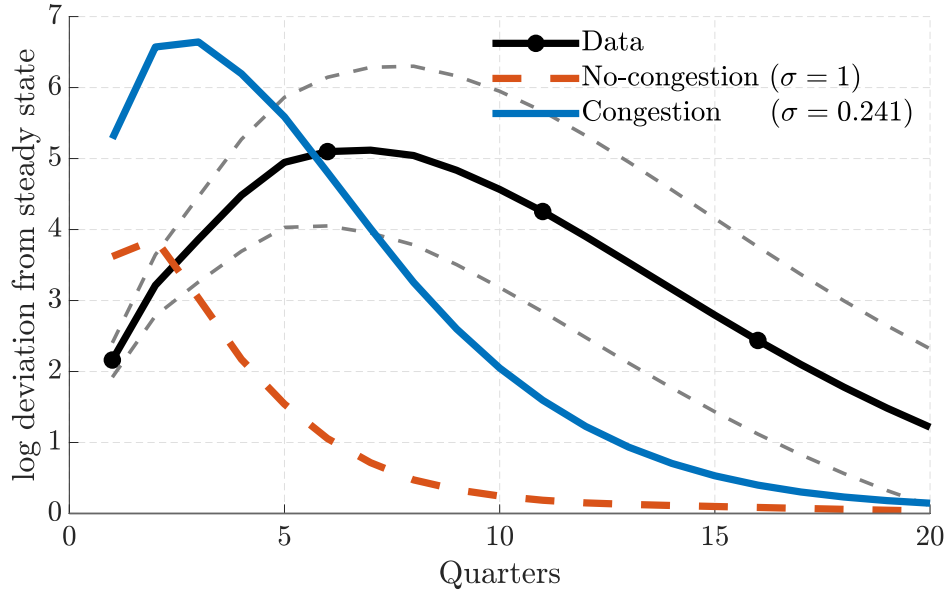


Notes: Panel (a) plots the average share of involuntary separations among EE and UE hires. The latter conditions on the separation reason from the last job before the current unemployment spell. Panel (b) plots the share of EE transitions that are involuntary. The time series are seasonally adjusted by taking out month dummies and for visually clarity are smoothed by taking backward-looking four-month moving averages. Source: 1996, 2001, 2004 and 2008 SIPP panels.

C Further Details on Identification of Congestion

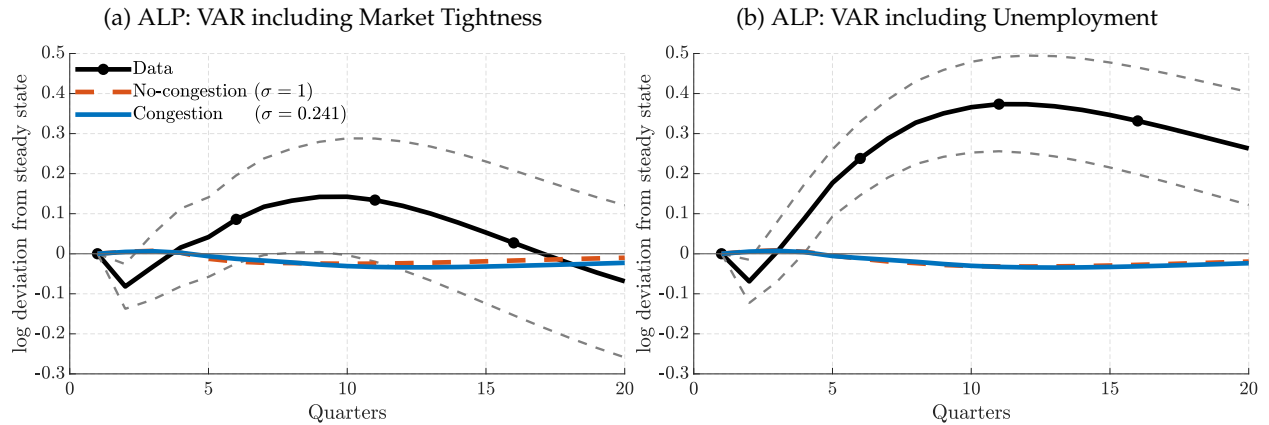
C.1 Additional Tables and Figures

Figure A14: IRF of Unemployment Rate to a Separation Rate Shock: Data and Models



Notes: The figure plots the empirical impulse response of unemployment rate to a separation shock (dashed lines are one standard deviation confidence bands), together with model responses. The red dashed line is the standard model with homogeneous workers ($\sigma = 1$). The blue solid line is our model under the preferred calibration ($\sigma = 0.241$).

Figure A15: IRF of Labor Productivity to a Separation Rate Shock: Data and Models



Notes: Panel (a) plots the impulse response of average labor productivity to a unit standard deviation job separation shock using the VAR model in Equation (7) with market tightness as the last variable. Panel (b) plots the same with unemployment rate as the last variable.

Table A3: Benchmarks: Elasticity of Substitution Parameters Estimated in the Literature

Paper	Production factors	Specification	Congestion Parameter
Mercan, Schoefer, Sedlacek (2021)	Workers indexed by periods since unemployment n_k	$Y = z (\sum_k \alpha_k n_k^\rho)^{1/\sigma}$	$\sigma = 0.241$
Krusell, Ohanian, Rios-Rull, Violante (2000)	High skill h and low skill l workers	$Y = Ak_s^\alpha (\mu l^\sigma + (1 - \mu)(\lambda k_c^\rho + (1 - \lambda)h^\rho)^{\frac{\sigma}{\rho}})^{\frac{1-\alpha}{\sigma}}$	$\sigma = 0.401$
Hagedorn, Manovski, Stetsenko (2016)	Capital structures k_s and capital equipments k_c		
Jeong, Kim, Manovskii (2015)	Worker experience E and labor L	$Y = A(L^\mu + \delta E^\mu)^{1/\mu}$	$\mu = -2.95$
Borjas (2003)	Capital K and labor L	$Q = (\lambda_k K^\nu + \lambda_l L^\nu)^{1/\nu}$	$\eta = 0.714$
	Worker with education i and experience j , L_{ij}	$L = (\sum_i \theta_i L_i^\rho)^{1/\rho}$, $L_i = (\sum_j \alpha_{ij} L_{ij}^\eta)^{1/\eta}$	$\rho = 0.231$
Autor, Katz, Kearney (2008)	College N_c and high school N_h equivalent workers	$Q = [\alpha(aN_c)^\rho + (1 - \alpha)(bN_h)^\rho]^{1/\rho}$	$\rho = 0.363$
Card, Lemieux (2001)	High school and college labor of different age groups H_j and C_j	$Y = (\theta_H H^\rho + \theta_C C^\rho)^{1/\rho}$ $H = \sum_j (\alpha_j H_j^\eta)^{1/\eta}$, $C = \sum_j (\beta_j C_j^\eta)^{1/\eta}$	$\rho = 0.091 - 0.375$ $\eta = 0.75 - 0.83$

Notes: This table presents a meta study of existing estimates of elasticities of substitution in CES aggregate production functions with different labor types (of various kinds), reformulated analogously to our congestion parameter σ .

C.2 Robustness of Identification of Separation Shocks using Time-Series Variation

The main text uses a three-variate VAR to identify exogenous separation shocks, which are crucial for quantifying our congestion mechanism. In particular, the response of labor market tightness to the separation shock, identified recursively using a Cholesky decomposition, is the key moment that pins down our preferred value of σ , which governs the extent of congestion.

More so than in cross-sectional studies, shocks other than labor productivity may be correlated with separation rate shifts in the aggregate time series (see Uhlig, 2005, for standard concerns with the VAR approach). After all, ALP is smooth and not very cyclical (see, e.g., Shimer, 2005; Mitman and Rabinovich, 2020; Galí and Van Rens, forthcoming). In fact, in canonical models of endogenous separations (Mortensen and Pissarides, 1994), the same surplus shock that drives hiring fluctuations, drives separations. At the same time, however, separation and job finding rates exhibit considerable independent variation (see, e.g., Shimer, 2012a), and there exist theories of separation rate fluctuations without any connection to job surplus fluctuations (e.g., Golosov and Menzio, 2020). Similarly, reallocation shocks (Lilien, 1982) may shift new and old jobs' values in a directly affected sector, with the absorption of the freed-up labor to be done in a sector in which, e.g., TFP has not changed.

To address these concerns, this section assesses the role of omitted shocks in our estimated separation rate process. In particular, we study the leading drivers of business cycles in the macro literature: shocks to utilization-adjusted total factor productivity (Fernald, 2014a), credit spreads, (Gilchrist and Zakrajšek, 2012a), discount factors (Hall, 2017a), uncertainty (Jurado, Ludvigson, and Ng, 2015a), and monetary policy (Romer and Romer, 2004; Wieland and Yang, 2020a). We find that these shocks have essentially no predictive power for the separation shocks identified by our VAR. Moreover, controlling for these shocks leaves the specific time-path of our separation shocks essentially unchanged.¹⁰ We conclude that the leading candidates of observable shocks are unlikely to confound our estimation of the congestion dynamics.

C.3 Data for Alternative Shocks

We now describe the data used for our analysis. The three-variate VAR is the same as in the main text, described in Section 1. The data for the other macroeconomic shocks are described below.

Total Factor Productivity Shocks. We take the utilization-adjusted quarterly measure of total factor productivity (`dtfp_util`) from Fernald (2014a). The sample period for this shock is 1976Q1 – 2019Q4.

Financial Shocks. We use the “Gilchrist-Zakrajšek” credit spread as measured in Gilchrist and Zakrajšek (2012a). The sample covers 1976Q1 – 2010Q3.

Discount Factor Shocks. We use the discount factor shocks estimated by Hall (2017a), using the Shiller price index. The sample period is 1976Q1 – 2015Q2.

Uncertainty Shocks. We use the one-quarter-ahead macroeconomic uncertainty shocks estimated by Jurado, Ludvigson, and Ng (2015a). The sample period for this shock is 1976Q1 – 2019Q4.

¹⁰An alternative route would be to include those shocks in the empirical VAR. Since our theoretical model will not feature those shocks, we do not pursue this route. We suspect that our results will be similar, since the VAR, intuitively, captures the residual variation of labor market tightness with separation shocks.

Monetary Policy Shocks. We use the monetary policy shocks proposed by Romer and Romer (2004) and as updated by Wieland and Yang (2020a). The sample period for this shock is 1976Q1 – 2007Q4.¹¹

C.4 Separation Shocks and Other Macroeconomic Disturbances

To ascertain whether our estimated separation shocks are not simply reflecting effects of omitted variables, we regress them on the range of macroeconomic shocks described above. Specifically, we estimate

$$(A12) \quad \delta_t = \alpha_j + \sum_{s=0}^p \beta_{j,s} x_{j,t-s} + \eta_{j,t},$$

where $x_{j,t}$ indicates a structural shock in period t , where j denotes one of the five structural shocks (TFP, financial, discount factor, uncertainty and monetary policy). We choose $p = 4$, thereby considering the contemporaneous impact of the structural shocks as well as up to four of their quarterly lags.

In addition to estimating the individual impact of each of the macroeconomic shocks, we also consider their joint effect by estimating

$$(A13) \quad \delta_t = \tilde{\alpha}_j + \sum_{j=1}^5 \sum_{s=0}^p \tilde{\beta}_{j,s} x_{j,t-s} + \eta_t.$$

In all the above cases, we always estimate the regressions on the maximum sample size allowed by the data.

Table A4 presents the adjusted R^2 from each of the specifications above. The results suggest that the separation shocks identified by our three-variate VAR are in fact *not* driven by other (omitted) structural shocks that are independently identified outside of our VAR. The highest explanatory power is obtained by considering discount factor shocks, but even there the adjusted R-square is only 1.6%.

Table A4: Separation Shocks and Other Disturbances: Adjusted R-squared

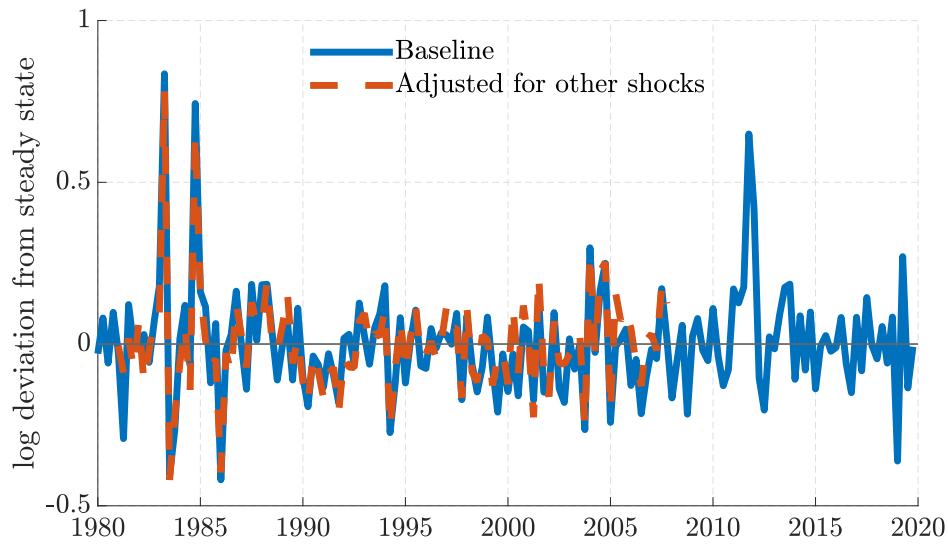
	TFP	Financial	Discount	Uncertainty	Monetary Policy	Joint
R^2	-0.006	0.003	0.016	-0.007	-0.018	-0.096
# of obs.	156	119	138	156	108	108
# of coefs.	6	6	6	6	6	26

Notes: The top row reports the adjusted R-square from the individual regressions (A12) for the five different macroeconomic shocks and the “joint” regression in Equation (A13). “TFP” is the utilization-adjusted total factor productivity (Fernald, 2014a), “financial” is the “Gilchrist-Zakrajšek” credit spread (Gilchrist and Zakrajšek, 2012a), “discount” is the discount factor shock based on the Shiller price index (Hall, 2017a), “uncertainty” is the one-quarter-ahead macroeconomic uncertainty (Jurado, Ludvigson, and Ng, 2015a) and “monetary policy” is taken from Wieland and Yang (2020a). The second and third rows report, respectively, the number of observations and estimated parameters in each regression.

Figure A16 shows how the separation shocks estimated in the main text change when controlling for all of the above macroeconomic shocks using the regression model in Equation (A13).

¹¹An alternative approach is to identify monetary policy shocks using high-frequency identification as in, e.g., Gürkaynak, Sack, and Swanson (2005); Gorodnichenko and Weber (2016); Gertler and Karadi (2015). However, these shock series cover a considerably shorter sample period.

Figure A16: Separation Shocks: Baseline and Adjusted for Identified Shocks



Notes: The figure shows the baseline separation shocks estimated in Section 1 and those shocks “adjusted for other disturbances” using the regression model in Equation (A13), where the plotted series is given by η_t .

The figure reveals that the estimated shocks are largely unchanged, as suggested by the slightly negative R^2 in Table A4.

D A Generalization of the Baseline Model: Types vs. Inputs

The baseline model in the main text assumes that every worker type k is a different input in production, i.e., $Y = z \left(\sum_{k=1}^K \alpha_k n_k^\sigma \right)^{\frac{1}{\sigma}}$. In this appendix we generalize this setup by allowing for subsets of worker types $i \subset \mathcal{K}$ to be perfectly substitutable in production. That is, different types k are not necessarily separate worker types as inputs into production, i . Instead, an input type $i \in \mathcal{I} = \{1, \dots, I\}$ is defined by a set of worker types $\Omega_i \subset \mathcal{K}$ which are mutually exclusive, i.e., $\cap_i \Omega_i = \emptyset$. The production function in this setting is given by $Y = z \left(\sum_i \alpha_i n_i^\sigma \right)^{\frac{1}{\sigma}}$.

This setup of worker heterogeneity nests multiple cases. For example, if $I = 1$, then $\Omega_1 = \mathcal{K}$ and all worker types constitute one input type (homogeneous workers). Types do not matter for production, so that this case boils down to the standard DMP model with a redundant worker type evolution in the background. Another setup has low- and high-skilled workers, where the former become the latter after, e.g., three years of employment. In a quarterly calibration, this setup would be given by assuming $I = 2$ with $\Omega_1 = \{1, \dots, 12\}$ and $\Omega_2 = \{13, \dots, K\}$. As a final example, each worker type is a separate input type (as in the main text), in which case $I = K$, and $\Omega_i = \{i\}$ for $i = 1, \dots, K$.

The retailer buys $\{n_i\}_{i=1}^I$ units of output in a perfectly competitive market. This implies that the prices for these goods satisfy the static first order conditions:

$$(A14) \quad p_i = \alpha_i n_i^{\sigma-1} \frac{Y}{\sum_j \alpha_j n_j^\sigma} = \alpha_i s_i^{\sigma-1} \frac{1}{\sum_j \alpha_j s_j^\sigma} \frac{Y}{N},$$

where $s_i = n_i/N$ denotes the share of type- i workers in production, and $N = \sum_i n_i$ is aggregate employment.

The worker and firm values now reflect the fact that worker types themselves are not imperfect substitutes in production, but only through their position in the production sets $i(k)$. The model equations differ only in that worker heterogeneity is now indexed by $i(k)$, rather than k .

E Solution Method

This appendix provides details of the solution and estimation methods used in the paper. We begin by describing the computation of the steady state, which includes the distribution of worker types among the employed and unemployed. We then lay out the solution method for the dynamic model and for its estimation.

E.1 Steady State

Given our parameterization, in particular the matching of the steady state job finding and separation rates, and our assumption that all unemployed fall to $k = 1$, it is possible to compute the implied distribution of worker types without solving for the rest of the model. Specifically, the steady state distribution of employment across worker types and steady state unemployment can be solved from the following set of equations:

$$\begin{aligned} e_1 &= fu, \\ e_{k+1} &= e_k(1 - \delta) \quad \text{for } k = 1, \dots, K - 1, \\ u &= (1 - f)u + \delta \sum_k e_k. \end{aligned}$$

In addition, under our calibration ensuring that $p_k = 1$ for all k in steady state, it is possible to compute the steady state surplus values for each type. This result, in turn, also pins down the steady state value of labor market tightness via the free-entry condition in Equation (20). Finally, using the steady state distribution of employment levels, and again the assumption that $p_k = 1$ for all k in steady state, we can calculate the implied productivity weights α_k via

$$1 = p_k = a_k s_k^{\sigma-1} \frac{1}{\sum_{l=1}^K \alpha_l s_l^{\sigma}} \frac{Y}{N},$$

where $s_k = e_k / (\sum_{l=1}^K e_l)$, and where we normalize average labor productivity $Y/N = 1$.

E.2 Solution and Estimation with Aggregate Uncertainty

Our model features heterogeneity in worker types and two aggregate sources of uncertainty, z and δ . The employment distribution gives another set of endogenous state variables. The distribution is, however, described without approximation error by the masses of workers of each of the K types. Transitions between these types shown in Equation (10), which depend on the job finding and separation rates, describe the distributional movements over time.

Therefore, there is no need to revert to iterative procedures, as the law of motion for the distribution is known a priori. We solve the model using first order perturbation around its stationary steady state (i.e., including the employment distribution). The large number of state variables (the two aggregate shocks, the distribution of employment shares and the unemployment rate) do not impede the speed of the solution method as perturbation is not prone to the curse of dimensionality.

To compute business cycle statistics, we simulate the model 100 times for 176 quarters (the length of our empirical sample). For each simulation, we detrend the logarithms of all the variables using the HP filter with a smoothing parameter of 1,600. The reported statistics are then averages over the 100 simulations. This also applies to impulse responses, which are averages of the estimated VARs over the 100 simulations.

E.3 The Kalman Filter

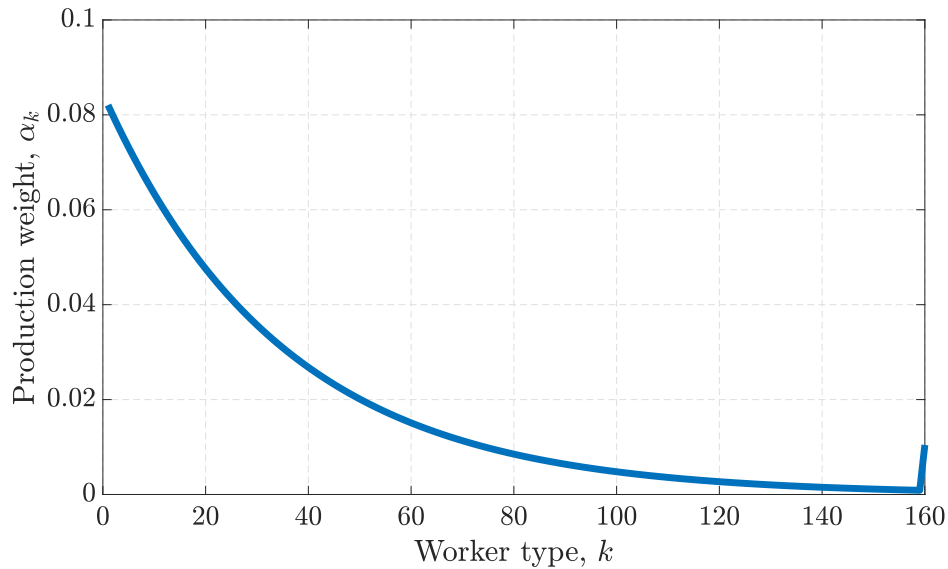
In addition, the linear nature of our solution allows us to estimate the model using the Kalman filter. Specifically, in Section 4.4 we use data on average labor productivity and the share of newly hired workers in employment to estimate the time path of the two aggregate shocks consistent with these two time series and our parameterization. The model structure then implies a particular time path for all model variables. We use this property in Section 4.4 to calculate the contribution of congestion unemployment to the variation in observed unemployment fluctuations. Figure A24 shows the time paths of other labor market variables implied by our estimation.

F Details of the Baseline Parameterization: Homogeneous Steady State Marginal Products Across Types

The main text describes the parameterization of the model, including that of the production weights α_k for different worker types. These are set such that the respective marginal products, p_k , are equal to 1 for all k . Hence, all worker types have the same (fundamental) surplus in steady state.

Figure A17 visualizes the calibrated values of the relative productivities. Their pattern mimics that of employment shares. Relatively abundant types, such as worker type $k = 1$, would be characterized by a lower marginal product unless its abundance is offset by a higher relative productivity weight α_1 . The spike at $k = K$ is due to the fact that this type is an absorbing state and therefore employment in this type is somewhat higher than in $k = K - 1$.

Figure A17: Relative Worker Productivities in the Congestion Model



Notes: The figure plots the relative weights in production, α_k , in the congestion model with $\sigma = 0.241$. The spike at $k = K (= 160)$ reflects the fact that it is an absorbing state.

G Alternative Calibration: Small Surplus/“High b ”

It is well understood that low fundamental surplus values help amplify the effects of productivity shocks and generate realistic unemployment fluctuations (see e.g., Ljungqvist and Sargent, 2017; Hagedorn and Manovskii, 2008). In this section, we consider an alternative calibration without congestion ($\sigma = 1$) with low surplus.

We calibrate most of our parameters as in the main text, except for the flow value of unemployment b , which is set such that the model matches the volatility of labor market tightness. We consider a version with and without separation shocks. The implied value of b is 0.96 in the case without separation shocks.

Results are presented in Table A5. While the model without separation shocks matches—by construction—the volatility of labor market tightness, it fails on the cyclicity of UE flows, for the same reasons as discussed in Section 1: separation shocks are necessary to match the countercyclical nature of UE flows. In the case with separation shocks, the model matches well the volatility of essentially all labor market variables. In addition, the model now also matches the countercyclicity of UE flows, albeit to a lesser extent than in the data. However, it grossly fails in the response of labor market tightness to a separation shock, as the standard model with separation rate shock discussed in the main text.

Figure A18 shows the empirical response of labor market tightness to a separation shock, with that of the model without congestion but with a low fundamental surplus and separation shocks. As in the standard model without congestion, there is essentially no response of labor market tightness to a separation shock. This key result does not change with a low fundamental surplus.

Steady State Elasticities. To understand this result further, we conduct a version of the analysis in Ljungqvist and Sargent (2017), but this time for separation shocks. In order to see whether separations have a sizable impact on hiring, we derive the elasticity of labor market tightness with respect to separations. Following Ljungqvist and Sargent (2017), we cast our model in continuous time in which case the hiring condition can be written as

$$(A15) \quad r + \delta = \frac{(z - b)(1 - \phi)q(\theta)}{\kappa} - \phi f(\theta),$$

where r is the interest rate such that $\beta = 1/(1 + r)$. Taking z as given and totally differentiating Equation (A15) with respect to δ and θ gives

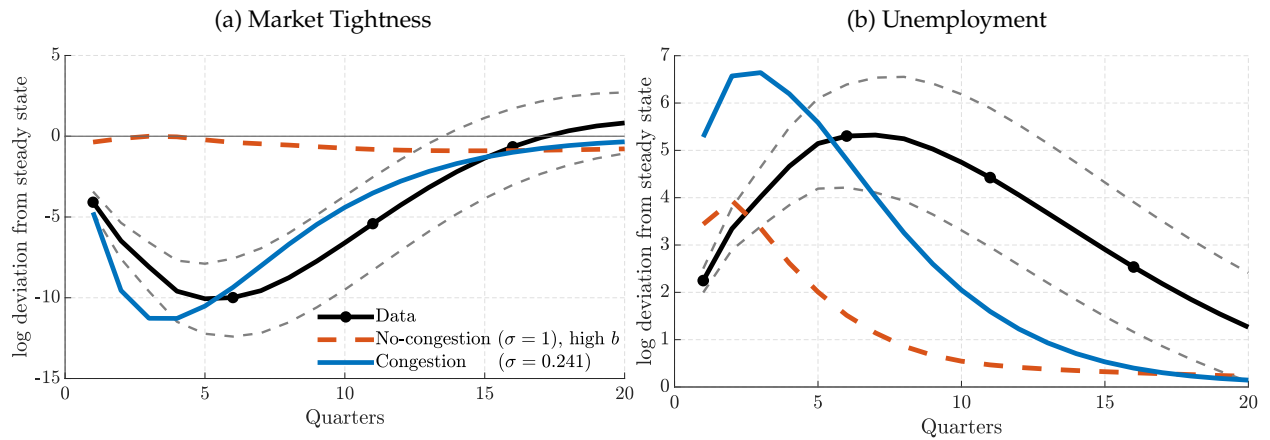
$$(A16) \quad \begin{aligned} d\delta &= \frac{(z - b)(1 - \phi)q'(\theta)}{\kappa} d\theta - \phi f'(\theta) d\theta \\ &= -[\mu(r + \delta) + \phi f(\theta)] \frac{d\theta}{\theta}. \end{aligned}$$

Rearranging the above, we can then write the elasticity of θ with respect to δ as

$$(A17) \quad \epsilon_{\theta, \delta} = \frac{d\theta/\theta}{d\delta/\delta} = -\frac{\delta}{\mu(r + \delta) + \phi f(\theta)} = -\Upsilon^{\text{Nash}} \frac{\delta}{r + \delta + \phi f(\theta)},$$

where $\Upsilon^{\text{Nash}} = \frac{r + \delta + \phi f(\theta)}{\mu(r + \delta) + \phi f(\theta)}$ is the scaling factor, which multiplies the fundamental surplus, derived in Ljungqvist and Sargent (2017). As discussed in Ljungqvist and Sargent (2017), reasonable calibrations of the standard search and matching model results in $\Upsilon^{\text{Nash}} \approx 1$. Moreover, these calibrations also result in the denominator in Equation (A17) being roughly equal to one half.

Figure A18: Impulse Responses to a Separation Shock: No-Congestion, Low-Surplus Model



Notes: The figure plots the impulse responses of labor market tightness and unemployment rate to a separation shock in the data and model, which is calibrated under a low fundamental surplus (e.g., Hagedorn and Manovskii, 2008) and includes countercyclical separation shocks.

In conclusion, the standard model features labor market tightness which is largely insensitive to separation shocks, with an elasticity of around -2δ . Moreover, this elasticity is *independent* of the fundamental surplus. This is precisely the reason why even a calibration with a low fundamental surplus cannot replicate the empirical response of labor market tightness to separation shocks.

Table A5: Business Cycle Properties: No-Congestion, Low-Surplus Model

	<i>ALP</i>	<i>f</i>	δ	<i>u</i>	<i>v</i>	θ	<i>UE/E</i>
<i>Panel A: Low Fundamental Surplus Model Without Separation Shocks</i>							
Standard deviation	0.010	0.064	0	0.052	0.199	0.230	0.049
Autocorrelation	0.706	0.706	0	0.844	0.596	0.706	0.311
Correlation matrix							
<i>ALP</i>	1						
<i>f</i>	0.999	1					
δ	0	0	1				
<i>u</i>	-0.647	-0.648	0	1			
<i>v</i>	0.980	0.981	0	-0.486	1		
θ	0.999	1.000	0	-0.648	0.981	1	
<i>UE/E</i>	0.476	0.476	0	-0.270	0.477	0.476	1
<i>Panel B: Low Fundamental Surplus Model With Separation Shocks</i>							
Standard deviation	0.010	0.064	0.082	0.090	0.177	0.227	0.068
Autocorrelation	0.691	0.689	0.560	0.825	0.558	0.689	0.623
Correlation matrix							
<i>ALP</i>	1						
<i>f</i>	0.999	1					
δ	-0.413	-0.430	1				
<i>u</i>	-0.674	-0.684	0.699	1			
<i>v</i>	0.933	0.929	-0.197	-0.368	1		
θ	0.999	1.000	-0.430	-0.684	0.929	1	
<i>UE/E</i>	0.005	-0.001	0.266	0.455	0.229	-0.001	1

Notes: *ALP*, *f*, δ , *u*, θ and *UE/E* indicate, respectively, average labor productivity, the job finding rate, separation rate, unemployment rate, labor market tightness, and share of new hires in employment. Panel A reports values from the model with a constant separation rate, Panel B reports the same for the model with countercyclical job separation shocks. All variables have been logged and the empirical cyclical components have been extracted using the HP-filter with a smoothing parameter of 1,600.

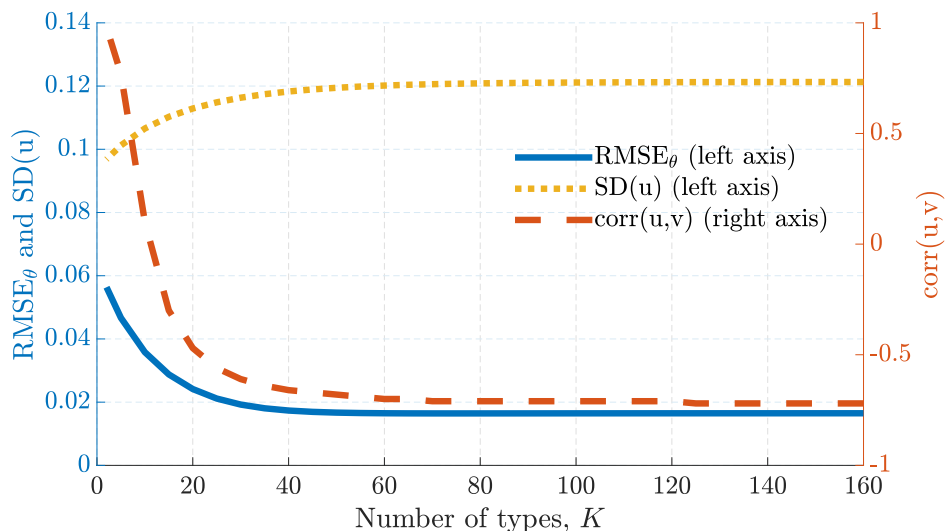
H Robustness of Model Performance to the Number of Worker Types

In the baseline model, we assume a maximum of $K = 160$ worker types. This means that workers gradually progress through different types while employed and remain at the highest rung only after 40 years of continuous employment in a quarterly calibration. In this section, we show that our results are robust to considerably reducing K .

Specifically, we solve and simulate our model for $K = 2, 3, \dots, 160$ and plot the corresponding standard deviation of unemployment, slope of the Beveridge curve ($\text{corr}(u, v)$) and the root mean squared error between the model and empirical impulse responses of labor market tightness to a job separation shock for each value of K . While the former two are key model outcomes, the latter is a measure used to parameterize the congestion parameter, σ . Note that in this exercise we neither recalibrate σ (but keep it at the value in the baseline model with $K = 160$), nor the size of the shocks.¹²

Figure A19 shows the three measures as a function of the number of types K on the horizontal axis. Our baseline results are obtained on the far right of the figure, at $K = 160$. As the figure makes clear, our results are essentially unaffected even if the number of types K is reduced from 160 to about 30, i.e. even if workers “grow out” of their cohort after about 7 years, rather than 40.

Figure A19: Volatility of unemployment, slope of the Beveridge curve and model fit vs K



Notes: The figure plots the standard deviation of unemployment, the correlation between unemployment and vacancies (i.e. the slope of the Beveridge curve) and the distance between model and empirical IRFs of labor market tightness to an innovation in the job separation rate for each of the of maximum number of worker types K .

Reducing the number of types further below 30 leads to a quick deterioration of the model performance. With the extreme case of only $K = 2$ types (far left values), we effectively retain the “standard” search and matching model with separation shocks, which completely fails in generating a strongly negatively sloped Beveridge curve. In fact, in the case of $K = 2$ worker types, the correlation between unemployment and vacancies is almost 1. Moreover, this model fails to generate congestion as measured by the effect of labor market tightness to separation rate shocks, as indicated by the RMSE curve. Hence, the region where K yields low levels of amplification is

¹²We do, however, recalibrate the production weights, α_k , such that the marginal product of each worker type p_k still remains to be equal to 1 as in the baseline.

exactly the region where the model starts to fail on other margins too; this is due to the absence of congestion, and may require recalibrating σ (which, in turn, would recover similar amplification even with lower K). We here illustrate that even with the original σ , a wide range of K leaves our results unchanged.

To understand these patterns, it is useful to express the surplus of newly hired workers as the discounted present value of *future* productivity levels (net of outside options, b). In particular, in our model the surplus of a worker of type k can be expressed as (see Equation (23)):

$$(A18) \quad S_{k,t} = p_{k,t} - b + \beta \mathbb{E}_t(1 - \delta_{t+1})S_{k+1,t+1} - \beta \mathbb{E}_t(1 - \delta_{t+1})f(\theta_t)\phi S_{1,t+1}.$$

Focusing on the steady state and iterating the above equation forward (in terms of worker cohorts, k), we can express the surplus of a newly hired worker as

$$(A19) \quad S_1 = \sum_{k=1}^{\infty} (\beta(1 - \delta))^{k-1} (p_k - b) - \sum_{k=1}^{\infty} (\beta(1 - \delta))^k f(\theta)\phi S_1.$$

As in the standard search and matching model, the surplus of newly hired workers determines hiring decisions and, therefore, the pattern of vacancies. In our baseline model, a separation shock incipiently increases unemployment and subsequently the mass of new hires in aggregate production, which leads to a reduction in $p_{1,t}$ through our congestion mechanism. In addition, as we explain in the main text, workers cannot escape the curse of an abundant cohort because all newly hired workers who remain in employment become $k = 2$ type workers in $t + 1$, $k = 3$ type workers in period $t + 2$ and so on. Only after reaching the final type $k = K$ do cohorts “mix”. Therefore, our model features strong cohort effects, which further reduce the incentives to hire because workers are expected to have depressed marginal products in the future as they cannot escape the abundant hiring cohort for up to $K = 160$ quarters.

As we reduce K , workers can escape their abundant recession cohort sooner. Whether or not the reduction in K affects the fluctuations in the total surplus of newly hired workers depends on a number of issues: how quickly workers escape their cohort (k), how plentiful is the absorbing type (K), how strongly its marginal product changes, the strength of discounting, and also the persistence of the hiring boom (as workers reaching the K state will benefit from their relative scarcity compared to younger cohorts). This is a quantitative question and it turns out that under our baseline calibration, the results are largely unchanged for K between about 30 and 160.

To understand the horse-race between these effects further, consider the extreme case of $K = 2$ and, as the first case, a persistent hiring burst. A separation shock reduces the employment stocks of both types, but because of full type loss in unemployment, only $k = 1$ types become abundant at the time of hiring. However, $k = 2$ types remain scarce owing to the hiring burst into the $k = 1$ type. Therefore, the present-value surplus of newly hired workers depends on a depressed $p_{1,t}$ in the first period and an increased $p_{2,t+1}$ in the next period and thereafter, as the economy keeps absorbing new hires. Given that $k = 2$ is the absorbing highest worker type rung, a worker spends the vast majority of their employment in that type and the surplus of newly hired workers is dominated by the increase in p_2 . As a result, the surplus of new hires falls by less than in a model with higher K . As the second case, now consider $K = 2$ with a transitory hiring burst (lasting only the first period). Then, even with $K = 2$, congestion effects are larger as hiring returns to normal once the $K = 2$ type enters the $k = K = 2$ type, which is relatively abundant once the cohort enters it.

Finally, the effects described above depend on the relative amounts of time spent in abundant and scarce worker cohorts, rather than the absolute number of types. For simplicity, we have

assumed that types correspond to quarters, and that workers move up by a type each model period. Alternatively, one could assume that workers move types, e.g., once every five years, i.e. we could slow down the type upgrade process without increasing K . In such a case, even a relatively small number of types K may allow for strong cohort effects and recover our baseline results (especially when recalibrating σ as in the main text).

I Business Cycle Statistics Including Full Correlation Matrices

For compactness, Table 2 in the main text only reports correlations with unemployment. Here, we additionally report the tables with the full correlation matrices. The tables are ordered as the panels in Table 2.

Table A6: Business Cycle Properties in the Data

	<i>ALP</i>	<i>f</i>	δ	<i>u</i>	<i>v</i>	θ	<i>UE/E</i>
Standard deviation	0.010	0.053	0.067	0.103	0.126	0.229	0.067
Autocorrelation	0.746	0.871	0.773	0.934	0.926	0.936	0.836
Correlation matrix							
<i>ALP</i>	1						
<i>f</i>	0.042	1					
δ	-0.415	-0.715	1				
<i>u</i>	-0.112	-0.931	0.848	1			
<i>v</i>	0.309	0.874	-0.869	-0.934	1		
θ	0.223	0.917	-0.875	-0.980	0.986	1	
<i>UE/E</i>	0.173	-0.722	0.567	0.833	-0.711	-0.783	1

Notes: *ALP*, *f*, δ , *u*, θ and *UE/E* indicate, respectively, average labor productivity, the job finding rate, separation rate, unemployment rate, labor market tightness and the share of new hires in employment. All variables have been logged and detrended using the HP-filter with a smoothing parameter of 1,600.

Table A7: Business Cycle Properties in the No-Congestion Model without Separation Shocks

	<i>ALP</i>	<i>f</i>	δ	<i>u</i>	<i>v</i>	θ	<i>UE/E</i>
Standard deviation	0.010	0.004	0	0.003	0.013	0.015	0.003
Autocorrelation	0.704	0.704	0	0.843	0.592	0.704	0.306
Correlation matrix							
<i>ALP</i>	1						
<i>f</i>	1.000	1					
δ	0	0	1				
<i>u</i>	-0.643	-0.643	0	1			
<i>v</i>	0.980	0.980	0	-0.481	1		
θ	1.000	1.000	0	-0.643	0.980	1	
<i>UE/E</i>	0.476	0.476	0	-0.272	0.476	0.476	1

Notes: *ALP*, *f*, δ , *u*, θ and *UE/E* indicate, respectively, average labor productivity, the job finding rate, separation rate, unemployment rate, labor market tightness and the share of new hires in employment. All variables have been logged and detrended using the HP-filter with a smoothing parameter of 1,600.

Table A8: Business Cycle Properties in the No-Congestion Model with Separation Shocks

	<i>ALP</i>	<i>f</i>	δ	<i>u</i>	<i>v</i>	θ	<i>UE/E</i>
Standard deviation	0.010	0.005	0.088	0.068	0.058	0.017	0.067
Autocorrelation	0.688	0.647	0.499	0.736	0.751	0.647	0.74
Correlation matrix							
<i>ALP</i>	1						
<i>f</i>	0.975	1					
δ	-0.441	-0.627	1				
<i>u</i>	-0.508	-0.665	0.916	1			
<i>v</i>	-0.306	-0.482	0.888	0.974	1		
θ	0.975	1.000	-0.627	-0.665	-0.482	1	
<i>UE/E</i>	-0.348	-0.402	0.413	0.739	0.747	-0.402	1

Notes: *ALP*, *f*, δ , *u*, θ and *UE/E* indicate, respectively, average labor productivity, the job finding rate, separation rate, unemployment rate, labor market tightness and the share of new hires in employment. All variables have been logged and detrended using the HP-filter with a smoothing parameter of 1,600.

Table A9: Business Cycle Properties in the Congestion Model—Baseline (Matching *UE/E*)

	<i>ALP</i>	<i>f</i>	δ	<i>u</i>	<i>v</i>	θ	<i>UE/E</i>	p_1
Standard deviation	0.010	0.059	0.122	0.121	0.102	0.207	0.067	0.055
Autocorrelation	0.688	0.897	0.530	0.836	0.857	0.897	0.742	0.772
Correlation matrix								
<i>ALP</i>	1							
<i>f</i>	0.443	1						
δ	-0.410	-0.509	1					
<i>u</i>	-0.463	-0.924	0.743	1				
<i>v</i>	0.348	0.922	-0.157	-0.716	1			
θ	0.443	0.996	-0.514	-0.940	0.909	1		
<i>UE/E</i>	-0.337	-0.930	0.392	0.865	-0.876	-0.940	1	
p_1	0.490	0.952	-0.431	-0.862	0.900	0.949	-0.973	1

Notes: *ALP*, *f*, δ , *u*, θ , *UE/E* and p_1 indicate, respectively, average labor productivity, the job finding rate, separation rate, unemployment rate, labor market tightness, the share of new hires in employment and marginal labor product of new hires. All variables have been logged and detrended using the HP-filter with a smoothing parameter of 1,600.

Table A10: Business Cycle Properties in the Congestion Model—Robustness (Matching EU & Participation)

	<i>ALP</i>	<i>f</i>	δ	<i>u</i>	<i>v</i>	θ	<i>UE/E</i>	p_1
Standard deviation	0.010	0.054	0.067	0.099	0.099	0.189	0.052	0.051
Autocorrelation	0.701	0.901	0.544	0.850	0.889	0.902	0.767	0.787
Correlation matrix								
<i>ALP</i>	1							
<i>f</i>	0.323	1						
δ	-0.419	-0.488	1					
<i>u</i>	-0.337	-0.941	0.693	1				
<i>v</i>	0.284	0.960	-0.241	-0.819	1			
θ	0.326	0.997	-0.491	-0.954	0.952	1		
<i>UE/E</i>	-0.240	-0.938	0.390	0.890	-0.913	-0.946	1	
p_1	0.414	0.950	-0.443	-0.882	0.926	0.948	-0.973	1

Notes: *ALP*, *f*, δ , *u*, θ , *UE/E* and p_1 indicate, respectively, average labor productivity, the job finding rate, separation rate, unemployment rate, labor market tightness, the share of new hires in employment and marginal labor product of new hires. All variables have been logged and detrended using the HP-filter with a smoothing parameter of 1,600.

Table A11: Business Cycle Properties in the Congestion Model—Robustness (Matching EU only)

	<i>ALP</i>	<i>f</i>	δ	<i>u</i>	<i>v</i>	θ	<i>UE/E</i>	p_1
Standard deviation	0.010	0.043	0.067	0.073	0.087	0.151	0.036	0.059
Autocorrelation	0.688	0.922	0.601	0.875	0.899	0.922	0.755	0.779
Correlation matrix								
<i>ALP</i>	1							
<i>f</i>	0.383	1						
δ	-0.435	-0.429	1					
<i>u</i>	-0.437	-0.923	0.696	1				
<i>v</i>	0.300	0.960	-0.166	-0.793	1			
θ	0.383	0.996	-0.431	-0.937	0.955	1		
<i>UE/E</i>	-0.323	-0.906	0.474	0.892	-0.842	-0.914	1	
p_1	0.468	0.918	-0.509	-0.885	0.848	0.913	-0.975	1

Notes: *ALP*, *f*, δ , *u*, θ , *UE/E* and p_1 indicate, respectively, average labor productivity, the job finding rate, separation rate, unemployment rate, labor market tightness, the share of new hires in employment and marginal labor product of new hires. All variables have been logged and detrended using the HP-filter with a smoothing parameter of 1,600.

J Alternative Calibration: Accounting for Labor Force Participation and Matching EU Flows

The baseline model calibrates separation shocks such that the model matches the observed fluctuations in the share of new hires in employment, UE/E , which are key to our congestion mechanism. However, as a result, the baseline model overpredicts the volatility of employment-to-unemployment (EU) flows, by overpredicting the volatility of EU separation rate δ .

In this appendix, we show that this inability to match both realistic new-hire employment shares and EU separations is primarily due to the missing non-participation margin in our two-state framework. We choose our two-state labor market framework for convenience and its direct comparability with canonical models in the literature (see, e.g., Shimer, 2005; Pissarides, 2009). However, two labor-market states mean that our framework attributes any flows into and out of non-participation (out of the labor force; OLF, or “O”, as we denoted nonemployment, comprising out of the labor and unemployment by “N”) to flows between employment and unemployment. This problem is common to all two-state models. See Elsby, Hobijn, and Sahin (2015) for the importance of the nonparticipation margin over the business cycle.

This quantitative extension still generates unemployment fluctuations that are 96% as volatile as in the data, and the Beveridge curve correlation of -0.819 , indicating that the success of the model is robust to alternative specification of worker flows. Therefore, our preferred specification remains the simple two-state model for convenience and its direct comparability with canonical models in this active literature (see, e.g., Shimer, 2005; Pissarides, 2009; Hagedorn and Manovskii, 2008; Ljungqvist and Sargent, 2017).

J.1 Clarifying the Problem

One consequence of the omitted third state and transitions into and out of it is that the law of motion for unemployment—which holds in the model at all times—does not hold for the empirical measures of f , δ and u :

$$(A20) \quad u_{t+1} = (1 - f_t)u_t + \delta_{t+1}(1 - u_t).$$

However, it is possible to compute an *implied* empirical measure of EU separation rates δ_{t+1}^{imp} consistent with the two-state law of motion of unemployment given by the above equation and the measured unemployment and job finding rates in the data.¹³ Specifically, we compute this implied process as

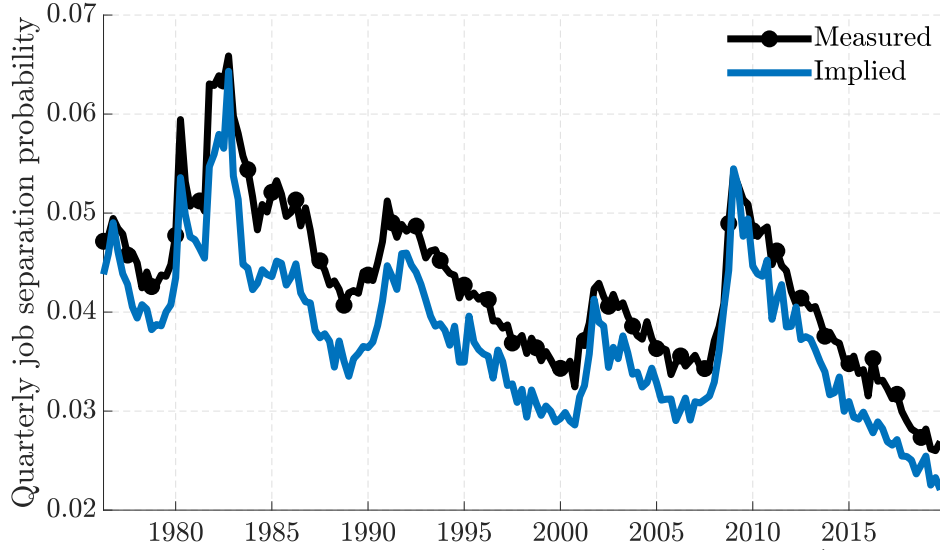
$$(A21) \quad \delta_{t+1}^{imp} = \frac{u_{t+1} - (1 - f_t)u_t}{1 - u_t}.$$

In words, this implied separation rate captures the two-state separation rate process that would, when feeding in the empirical job finding rate and the unemployment rate, exactly predict the empirical level of the next period unemployment rate.

Comparing the implied EU separation rate δ^{imp} with the actual EU separation rate δ permits a useful diagnostic: whenever δ^{imp} exceeds δ , it must be that out-of-steady-state transitions between OLF and E or U occurred that, on net, lowered empirical employment or raised unemployment by more than accounted for by EU transitions (δ) and UE transitions (f)—where these have been

¹³This procedure resembles that in Shimer (2005), who backs out the job finding rate using the law of motion for unemployment and a proxy for EU flows using short-term unemployment. In our case, the procedure is reversed, with the EU flows being backed out from the law of motion for unemployment given a measure of the job finding rate.

Figure A20: Separation Rate: Measured and Implied



Note: “Measured” δ refers to the empirical time series in the main text. “Implied” refers to δ^{imp} described above, based on the law of motion for unemployment, the unemployment rate and the job finding rate.

constructed on the basis of panel data measuring the transitions of workers between U and E states, i.e. measured EU and UE flows.

Figure A20 shows the time series of the measured and implied separation rates, i.e., δ and δ^{imp} . The implied separation rate is more volatile and less persistent compared to the measured one. This comparison highlights the tension between a two-state model of the labor market and directly measured flows in the data.

Below, we recalibrate the baseline model to account for the discrepancy described above. Subject to a recalibration of our key parameter, σ , the extended model delivers essentially the same quantitative results while, at the same time, matching the observed variation in EU flows.

J.2 Introducing Flows Into and Out of Non-Participation

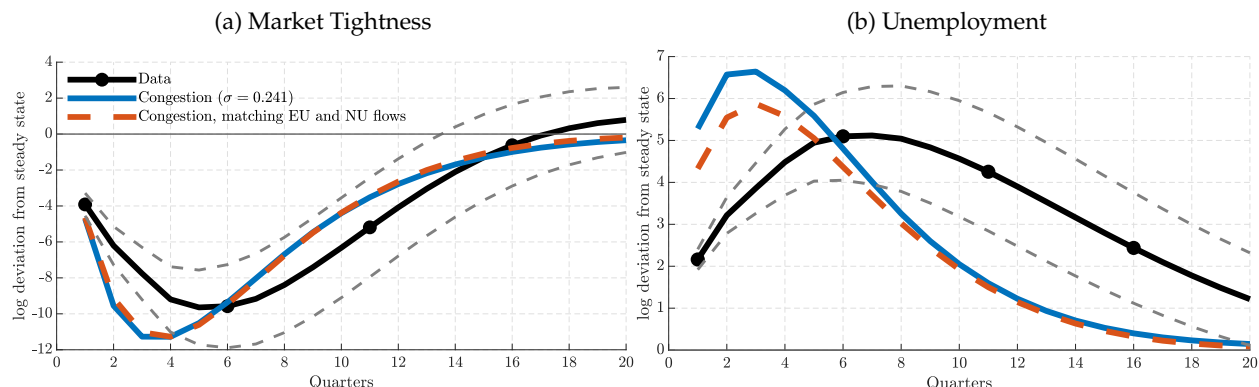
We now present an alternative model that quantitatively accounts for the presence of flows into and out of non-participation. To nevertheless retain the logic of our two-state model, we introduce *exogenous* net changes in the number of unemployed. In particular, the law of motion for the mass of unemployed of type $k = 1$ is given by

$$(A22) \quad u_{1,t} = (1 - f(\theta_{t-1}))u_{1,t-1} + \delta_t \sum_{k=1}^K e_{k,t} + OU_t,$$

where we have retained our assumption that all separated workers fall to the bottom of the ladder and become type $k = 1$. The new feature, compared to the baseline model, is the presence of OU_t flows, which reflects the possibility of (exogenous) changes in the unemployment pool proxying for flows into and out of OLF. Specifically, we assume that OU fluctuates according to the following process:

$$(A23) \quad OU_t = \rho_{OU}OU_{t-1} + \epsilon_{OU,t},$$

Figure A21: Impulse Responses to a Separation Shock: Baseline and Alternative Calibration of Separation Rate Process to Match EU Flows



Notes: The figure plots the impulse responses of labor market tightness and unemployment rate to a separation shock in the data and model, which is calibrated to match the business cycle patterns of EU flows.

where $\rho_{OU} \in (-1, 1)$ is a persistence parameter and $\epsilon_{OU,t} \sim N(0, \sigma_{OU}^2)$ are random shocks. This extension does not change the steady state of our model as OU flows are assumed to have zero mean.

J.3 Parameterized Model with Empirical δ Process and OU Flows

We parameterize the extended model in exactly the same way as the baseline model, except that instead of targeting UE/E flows, we directly parameterize the δ process to match the cyclical pattern of EU flows in the data.

In addition, we set ρ_{OU} and σ_{OU} to match the persistence and volatility of OU flows as a share of the labor force observed in the data, constructed as described in Appendix A.1.¹⁴ In addition, we allow for a correlation between ϵ_{δ} and ϵ_{OU} to match the observed correlation between $OU/(E + U)$ and the unemployment rate, which is 0.72.

Table A10 in Appendix I, and Panel E of Table 2 in the main text, show the business cycle statistics of the extended model. This model matches not only the volatility of average labor productivity, but now also that of EU flows—specifically, the δ process now has the same volatility as in the data (although we miss some of its persistence). Moreover, the extended model still delivers a large amount of amplification of shocks. Specifically, the volatility of unemployment is 96% that of the data and the Beveridge curve has a healthy correlation of -0.819 . Since we no longer target the UE/E fluctuations, they are now somewhat less volatile than in the data. But, the calibrated separation shocks together with the additional OU flows result in unemployment-to-employment flows being relatively close to what they are in the data.

In order to match the impulse response of labor market tightness to separation shocks, the extended model requires a σ of 0.08. Under this calibration, however, the extended model delivers essentially identical dynamics as the baseline model, as shown in Figure A21.

To conclude, the baseline model refined to match the volatility of the empirical separation rate process and extended for the possibility of (exogenous) flows into and out of non-participation

¹⁴Because of the assumed zero mean in the model, we match the persistence and volatility in levels, rather than logs. The average ratio $OU/(U + E)$ is 1.4%, with persistence of 0.57 and standard deviation of 0.001.

parameterized to match those observed in the data, has essentially identical amplification properties regarding labor market tightness and unemployment as the baseline model presented in the main text. While we choose to retain the standard two-state labor market model as our main specification, we conjecture that an explicit modelling of an endogenous non-participation choice would yield very similar results (provided that such a hypothetical model succeeds in matching the UE flows and congestion dynamics). Krusell et al. (2017) and Cairó, Fujita, and Morales-Jimenez (2020) present such richer models of worker flows for all three margins (but do not study congestion dynamics).

J.4 Ignoring OU Flows

We believe that accounting for flows from non-participation is important when targeting EU flows directly. Nevertheless, in this subsection we present results for the case when we target the cyclical pattern of EU flows, but ignore flows from out of the labor force.

Table A11 shows the business cycle statistics of our baseline model calibrated to match the cyclical pattern of EU flows, rather than that of UE/E. Here, the volatility of the model-implied series of UE/E flows is less than 50% of that in the data, and therefore the model underperforms the baseline in terms of the volatility of other labor market variables as it features an unrealistically low degree of congestion. For instance, the volatility of unemployment is about 3/4 of that in the data.

However, this model still outperforms the standard framework without congestion along several dimensions. Most notably, the model with congestion targeting EU flows does feature a strong Beveridge curve ($corr(u, v) = -0.79$). For this reason, the model also predicts a considerably more volatile labor market tightness ($SD(\theta) = 0.151$), compared to the model without congestion, but with separation shocks ($SD(\theta) = 0.017$).

K Deriving the Iso-congestion Curve

We generalize the production function in our baseline model and assume a function that takes the following form:

$$Y = (1 - x) \left(\sum_k \alpha_k^c (n_k^c)^\sigma \right)^{1/\sigma} + x \left(\sum_k \alpha_k^{nc} n_k \right).$$

In words, we assume that a share $1 - x$ of workers are subject to short-run congestion and the remaining share x of workers are not subject to congestion in final good production. Alternatively, fraction x of workers enter the k step in a way that replicates the skill structure at the point of hiring. Or, two final goods are produced, which are perfect substitutes but one uses linear production. Search is random, so a given hire is expected to be placed into the two functions with probabilities $1 - x$ and x , respectively.

Marginal Product of Labor. This new production function implies that the expected marginal product of a hire will be, when the congestion hire reaches type- k :

$$p_k = \frac{\partial Y}{\partial n_k} = (1 - x) \underbrace{\alpha_k^c n_k^{\sigma-1} \left(\sum_k \alpha_k^c n_k^\sigma \right)^{1/\sigma-1}}_{=p_k^c} + x \underbrace{\alpha_k^{nc}}_{=p_k^{nc}}.$$

Measure of Congestion. We are interested in how fast the marginal product of labor-type k changes with respect to the mass of employed workers of that particular type. To this end, we use the elasticity of the marginal product of labor with respect to the mass of workers of type k , ε_{p_k, n_k} .

First, we observe that the elasticity of p_k^{nc} with respect to n_k is zero, $\varepsilon_{p_k^{nc}, n_k} = 0$. Second, we calculate the elasticity of p_k^c with respect to n_k

$$\begin{aligned} p_k^c &= \alpha_k^c n_k^{\sigma-1} \left(\sum_k \alpha_k^c n_k^\sigma \right)^{1/\sigma-1} \\ \Rightarrow \varepsilon_{p_k^c, n_k} &= \frac{\partial p_k^c}{\partial n_k} \frac{n_k}{p_k^c} \\ &= (\sigma - 1) \left(1 - \frac{\alpha_k^c n_k^\sigma}{\sum_k \alpha_k^c n_k^\sigma} \right). \end{aligned}$$

Third, we use the property that if $z = x + y$, then the following identity holds for the elasticity of z :

$$\varepsilon_z = \frac{x}{x + y} \varepsilon_x + \frac{y}{x + y} \varepsilon_y.$$

Fourth, using this identity and the fact that $\varepsilon_{p_k^{nc}, n_k} = 0$, we derive our desired elasticity of marginal product with respect to worker mass:

$$\varepsilon_{p_k, n_k} = (\sigma - 1) \left(1 - \frac{\alpha_k^c n_k^\sigma}{\sum_k \alpha_k^c n_k^\sigma} \right) \frac{(1 - x) \alpha_k^c n_k^{\sigma-1} \left(\sum_k \alpha_k^c n_k^\sigma \right)^{1/\sigma-1}}{(1 - x) \alpha_k^c n_k^{\sigma-1} \left(\sum_k \alpha_k^c n_k^\sigma \right)^{1/\sigma-1} + x \alpha_k^{nc}}.$$

The Iso-congestion Curve. Our calibration ensures that $p_k^c = p_k^{nc} = 1$ for all k , therefore the last term above simplifies to the share of no-congestion workers $1 - x$. Our congestion measure then becomes

$$(A24) \quad \varepsilon_{p_k, n_k} = (1 - x)(\sigma - 1) \left(1 - \frac{\alpha_k^c n_k^\sigma}{\sum_k \alpha_k^c n_k^\sigma} \right).$$

Further, as $p_k^c = \alpha_k^c n_k^{\sigma-1} \left(\sum_k \alpha_k^c n_k^\sigma \right)^{1/\sigma-1} = 1$ for all k , we have $\alpha_k^c n_k^{\sigma-1} = \alpha_l^c n_l^{\sigma-1}$. This implies that $\alpha_k^c n_k^\sigma = \alpha_l^c n_l^{\sigma-1} n_k$. Summing over k , we get $\sum_k \alpha_k^c n_k^\sigma = \alpha_l^c n_l^{\sigma-1} N / n_l$. Then we obtain $s_l = \frac{n_l}{N} = \frac{\alpha_l^c n_l^\sigma}{\sum_k \alpha_k^c n_k^\sigma}$. Using this result in the elasticity expression above, we finally arrive at

$$(A25) \quad \varepsilon_{p_k, n_k} = (1 - x)(\sigma - 1)(1 - s_k).$$

To trace out the iso-congestion curve for $k = 1$, we solve for σ as a function of x given a level of elasticity $\bar{\varepsilon}_{p_1, n_1}$

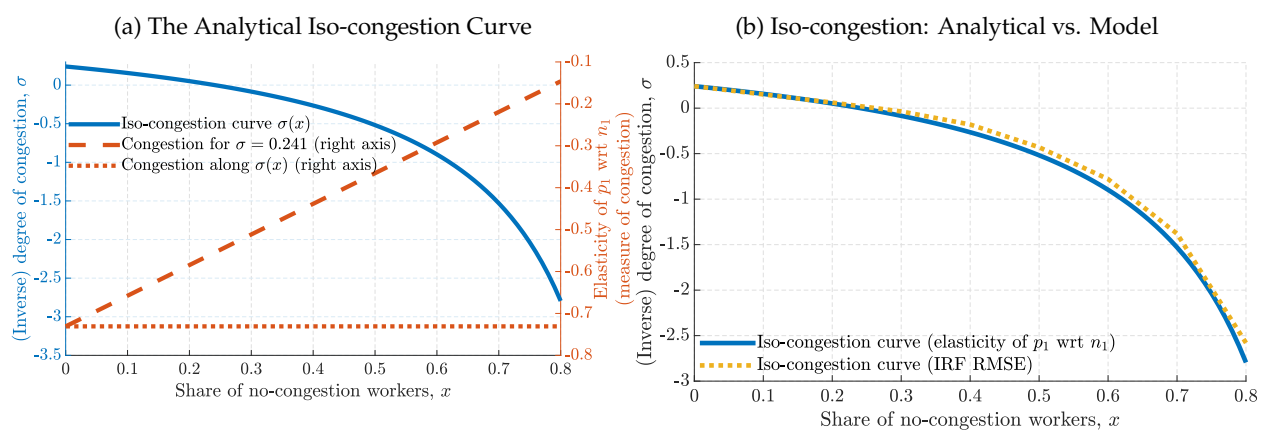
$$(A26) \quad \sigma(x) = 1 + \frac{\bar{\varepsilon}_{p_1, n_1}}{(1 - x)(1 - s_1)}.$$

The employment distribution over worker types is characterized by the job finding and separation rates, and the associated laws of motion for employment. Given our calibration strategy (i.e., ensuring $p_k = 1$ for all k), employment share of $k = 1$ workers, s_1 , then stays constant for different levels of the congestion parameter σ .

Figure A22 Panel (a) plots the iso-congestion curve derived in Equation (A26) starting from our baseline calibration of $x = 0$ and $\sigma = 0.241$. The figure makes clear that, as there is more weight on no-congestion workers in final good production, σ needs to be adjusted downward to maintain the same level of congestion as in our baseline calibration. In fact, if $\sigma = 0.241$ is held constant, higher levels of x lead to smaller congestion in production.

Panel (b) superimposes the iso-congestion curve we present in the main text based on the solution to the full dynamic model and on matching the IRF of labor market tightness to the separation rate shock in Figure 3. The figure reveals that, strikingly, the iso-congestion curve we derive analytically overlaps with the one implied by our calibrated model almost perfectly.

Figure A22: Iso-congestion Curves



Notes: Panel (a) plots the analytical iso-congestion curve as a function the share of no-congestion workers in production, x . It also includes the level of congestion as a function of x , as well as the constant level maintained along the iso-congestion curve. Panel (b) compares the analytical iso-congestion curve to the one we obtain solving our dynamic congestion model by matching the IRF of labor market tightness to the separation rate shock in Figure 3.

L Alternative Mechanism: Convex Hiring Costs

Our baseline model obtains congestion in hiring through diminishing returns in the production function. An alternative mechanism of congestion works through a countercyclical *hiring cost* besides the standard DMP vacancy maintenance costs, where, for our purposes, the cost is increasing in UE flows rather than in total hiring:¹⁵

$$(A27) \quad c(UE_t) = c_1 \cdot \left[\left(\frac{UE_t}{UE_{ss}} \right)^{c_2} - 1 \right].$$

This cost is zero in steady state; outside of steady state, hiring costs increase in UE flows ($c_1, c_2 > 0$).

The only difference from the standard DMP model is in the free-entry, zero-profit condition, which becomes

$$(A28) \quad \frac{\kappa}{q_t} + c(UE_{t+1}) = E_t [\beta(1 - \delta_{t+1})J_{t+1}].$$

In turn, we remove worker heterogeneity (essentially setting $\sigma = 1$ and setting the α_k 's to one to yield homogeneous marginal products). Hence, the hiring cost is the only source of congestion, and parameter c_2 guides its degree. We normalize $c_1 = 1$.

The model provides a promising avenue for generating countercyclical congestion by raising the costs of hiring during recessions, when UE flows are high.

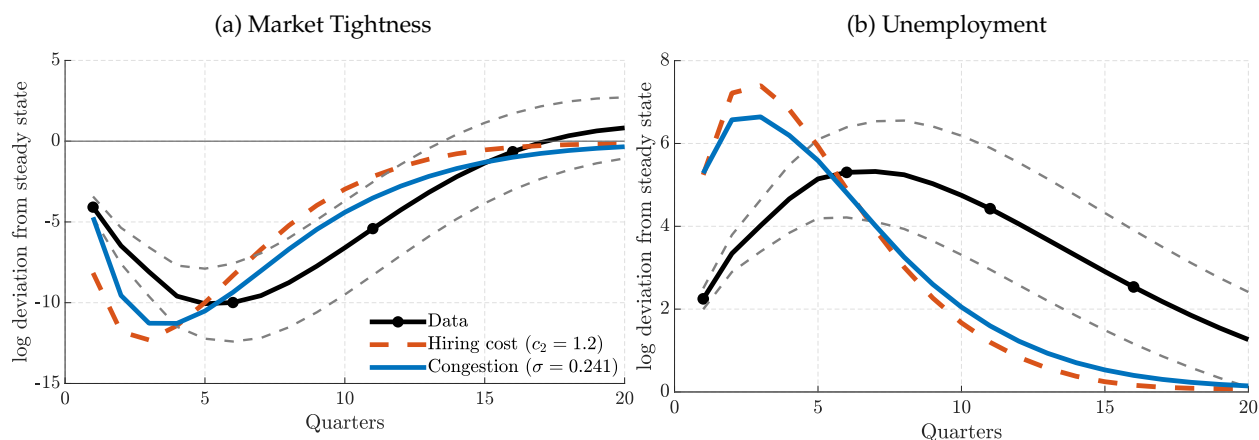
As with the production-function based congestion parameter σ , we now set c_2 such that the model minimizes the RMSE of the response of labor market tightness to separation shocks. Figure A23 shows that the fit of this model is excellent too, closely mirroring the IRF of our main specification in Figure 3. The estimated level of c_2 is 1.2.

The results are presented in Table A12. The model with convex hiring costs can indeed replicate well the volatility of labor market variables. The model also features a robustly negative Beveridge curve and countercyclical UE flows.

Moreover, the model based on convex hiring costs—as our production-based congestion model—is also reasonably sensitive to changes in labor market policies. The elasticity of unemployment with respect to changes in unemployment benefits is 2.59 as is our baseline, production-based congestion model, as it does not rely on a low fundamental surplus to explain labor market volatility. We note that, naturally, the model with convex hiring costs would not generate cyclical displacement costs that are persistent, for lack of cohort effects.

¹⁵Pissarides (2009); Silva and Toledo (2013) add a fixed costs of hiring, but it is not increasing in the amount of hires.

Figure A23: Impulse Responses to a Separation Shock: Convex Hiring Cost Model



Notes: The figure plots the impulse response functions of market tightness and unemployment to a unit standard deviation separation shock in the data, and the models of congestion through the production function and the convex hiring cost.

Table A12: Business Cycle Properties: Convex Hiring Cost Model

	ALP	f	δ	u	v	θ	UE/E
Standard deviation	0.010	0.061	0.118	0.129	0.096	0.219	0.067
Autocorrelation	0.691	0.855	0.536	0.845	0.856	0.855	0.840
Correlation matrix							
ALP	1						
f	0.505	1					
δ	-0.410	-0.726	1				
u	-0.474	-0.984	0.748	1			
v	0.518	0.967	-0.656	-0.907	1		
θ	0.505	1.000	-0.726	-0.984	0.967	1	
UE/E	-0.346	-0.873	0.316	0.858	-0.846	-0.873	1

Notes: ALP , f , δ , u , θ and UE/E indicate, respectively, average labor productivity, the job finding rate, separation rate, unemployment rate, labor market tightness and share of new hires in employment, for the model with convex hiring costs. All variables have been logged and the empirical cyclical components have been extracted using the HP-filter with a smoothing parameter of 1,600.

M Historical Decomposition: Additional Material

The main text shows how congestion-only unemployment contributed to the evolution of overall unemployment. In this section, we provide the same exercise also for TFP- and separation-driven unemployment. The estimated time paths of key labor market variables are presented in Figure A24.

The spirit of the decomposition exercise is exactly the same as in the main text and we specify the method below. In particular, we construct counterfactual unemployment rates generated by TFP shocks only u^z , which would arise in the TFP-shock-only models such as in Shimer (2005); Hall (2005); Hagedorn and Manovskii (2008) and generated by separation shocks only, u^δ . The corresponding equations that characterize these counterfactuals are, for u^z ,

$$(A29) \quad \begin{aligned} u_{t+1}^z &= (1 - f(\theta_t^z))u_t^z + \bar{\delta}(1 - u_t^z), \quad \kappa = q(\theta_t^z)\beta\mathbb{E}_t(1 - \bar{\delta})S_{1,t}^z \\ S_{k,t}^z &= z_t - b + \beta\mathbb{E}_t(1 - \bar{\delta})S_{k+1,t+1}^z - \beta\mathbb{E}_t(1 - \bar{\delta})f(\theta_t^z)\phi S_{1,t+1}^z \text{ for all } k, \end{aligned}$$

and, respectively, for u^δ ,

$$(A30) \quad \begin{aligned} u_{t+1}^\delta &= (1 - f(\theta_t^\delta))u_t^\delta + \delta_{t+1}(1 - u_t^\delta), \quad \kappa = q(\theta_t^\delta)\beta\mathbb{E}_t(1 - \delta_{t+1})S_{1,t}^\delta \\ S_{k,t}^\delta &= \bar{z} - b + \beta\mathbb{E}_t(1 - \delta_{t+1})S_{k+1,t+1}^\delta - \beta\mathbb{E}_t(1 - \delta_{t+1})f(\theta_t^\delta)\phi S_{1,t+1}^\delta \text{ for all } k. \end{aligned}$$

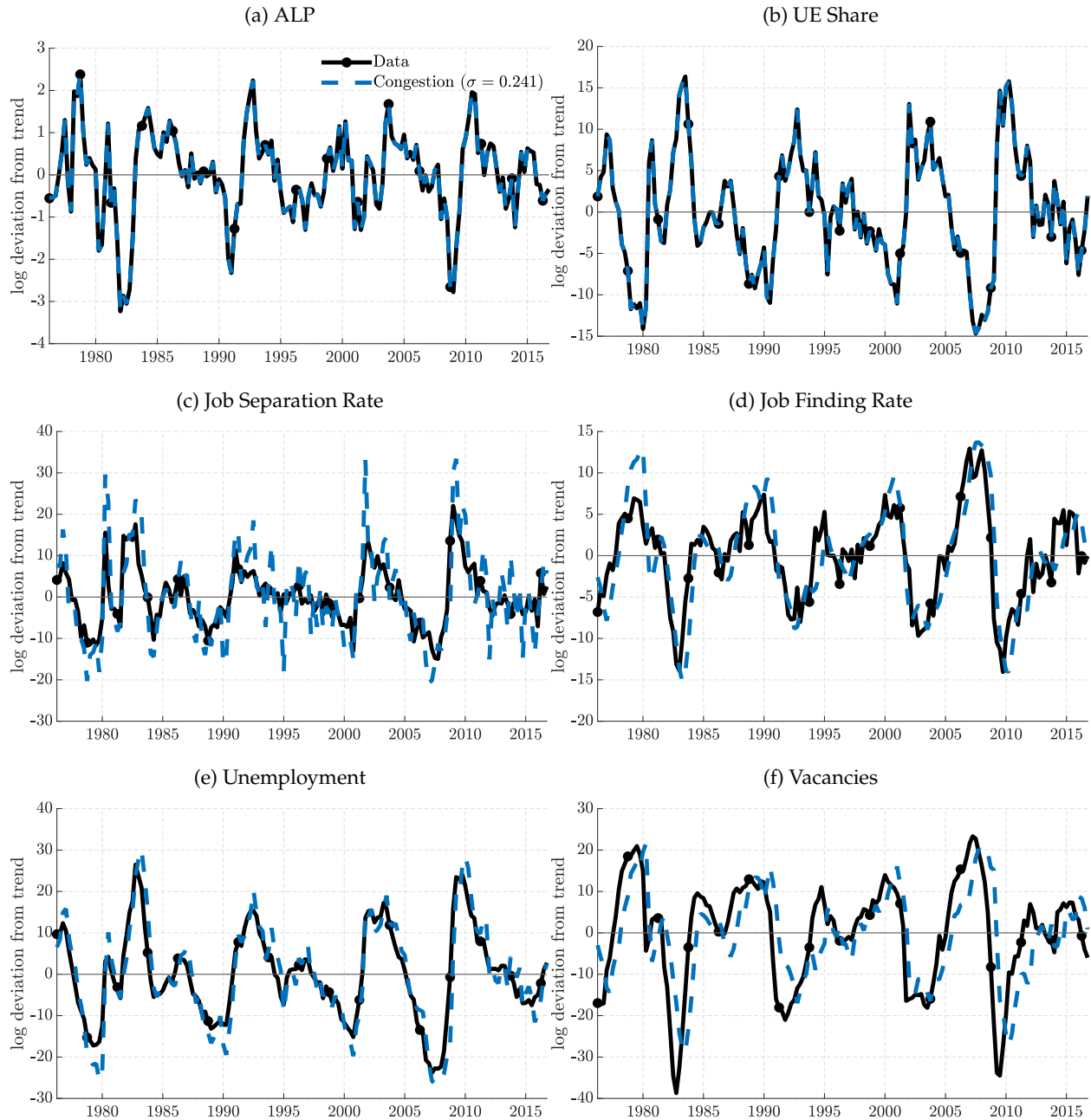
Figure A25 plots the associated time series of these counterfactual unemployment rates together with actual unemployment. Table A13 provides a set of business cycle statistics related to overall unemployment and the three counterfactuals.

Volatility. Table A13 quantifies the role of congestion-driven unemployment in US business cycles, reporting summary statistics of the actual and congestion-only unemployment rates. The congestion-only time series accounts for approximately 30% of the historical unemployment rate fluctuations in the United States. Its standard deviation is around 40% of the empirical one.¹⁶

Persistence and Internal Propagation. Congestion-driven unemployment is considerably more persistent than both TFP- and separation-driven unemployment. Its autocorrelation is 0.950, compared to 0.865 for TFP-driven and 0.825 for separation-driven unemployment rates. This additional persistence arises from the internal propagation mechanisms laid out in Section 4.3.

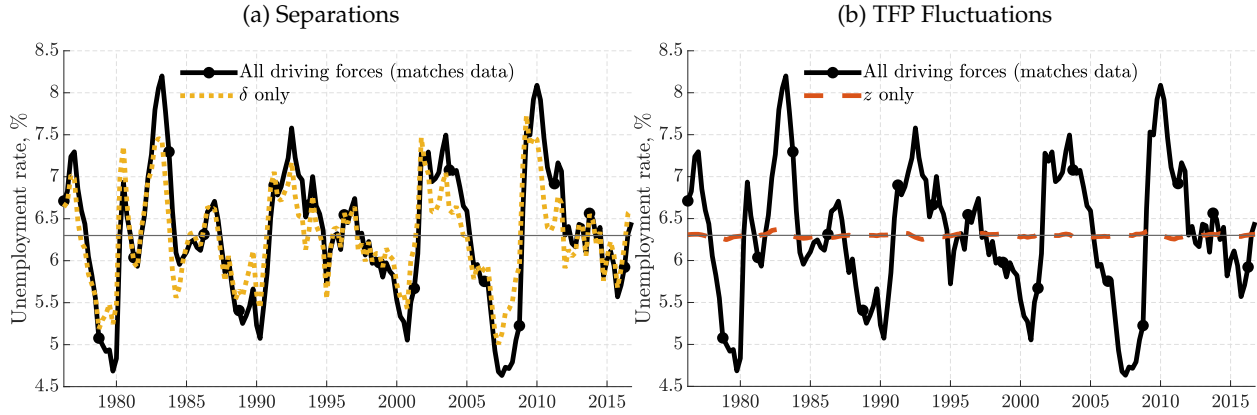
¹⁶As discussed in Section 4.1, our model matches UE flows by estimating a somewhat more volatile separation rate process. In Table A13, this property leads to the model exaggerating the share of unemployment fluctuations due to separation shocks. See Fujita and Ramey (2009) and Shimer (2012a) for the empirical contributions of the two transition rates to unemployment fluctuations in the US. A more realistic separation rate process will likely reduce the performance of the model in explaining overall unemployment fluctuations while leaving the contribution of congestion, which manifest itself on the hiring margin, unaffected, as long as that model generates realistic fluctuations in UE flows.

Figure A24: Time Paths of Labor Market Variables



Notes: The figure plots the estimated time paths of labor market variables using the Kalman Filter. Time series are logged and HP-filtered using a smoothing parameter of 1,600.

Figure A25: Unemployment Components



Notes: The figure plots actual, and counterfactual unemployment rates u^z and u^δ estimated using data on the cyclical components of average labor productivity and new hires as a share of employment. The counterfactual unemployment time series are based on Equations (A29) and (A30).

Table A13: Historical Decomposition of Unemployment: Model and Counterfactuals

	Baseline	Congestion only	z only	δ only
Standard deviation	0.124	0.050	0.004	0.089
Contribution to total	1	0.297	0.008	0.657
AR(1)	0.905	0.951	0.865	0.825
corr(x, y)				
Actual	1			
Congestion only	0.729	1		
z only	0.274	-0.264	1	
δ only	0.920	0.411	0.464	1

Notes: This table reports summary statistics for the unemployment rate time series generated using our model (which closely tracks the actual unemployment rate), and the counterfactuals from TFP shocks only, separation shocks only, and congestion only. "Contribution to total" shows $\text{cov}(u_{\text{base.}}, u_{\text{cf.}}) / \text{var}(u_{\text{base.}})$, where $u_{\text{base.}}$ is unemployment in our baseline model, while $u_{\text{cf.}}$ is the respective counterfactual unemployment rate.

Bibliography

- Blanchard, Olivier and Peter Diamond. 1990. "The Cyclical Behavior of the Gross Flows of US Workers." *Brookings Papers on Economic Activity* 1990 (2):85–155.
- Burda, Michael and Charles Wyplosz. 1994. "Gross Worker and Job Flows in Europe." *European Economic Review* 38 (6):1287–1315.
- Cairó, Isabel, Shigeru Fujita, and Camilo Morales-Jimenez. 2020. "The Cyclicity of Labor Force Participation Flows: The Role of Labor Supply Elasticities and Wage Rigidity." *Working Paper* .
- Elsby, Michael W. L., Bart Hobijn, and Aysegül Sahin. 2013a. "Unemployment Dynamics in the OECD." *The Review of Economics and Statistics* 95 (2):530–548.
- Elsby, Michael W. L., Bart Hobijn, and Aysegül Sahin. 2013b. "Unemployment Dynamics in the OECD: Dataset." *The Review of Economics and Statistics* 95 (2):530–548. URL <https://doi.org/10.7910/DVN/4BJC20/LFYZTF>.
- Faberman, Jason, Andreas Mueller, Aysegül Sahin, and Giorgio Topa. 2022. "Job search behavior among the employed and non-employed." *Econometrica* 90 (4):1743–1779.
- Fernald, John. 2014a. "A Quarterly, Utilization-adjusted Series on Total Factor Productivity." *Working Paper* .
- . 2014b. "A Quarterly, Utilization-adjusted Series on Total Factor Productivity: Dataset." *Working Paper* URL <https://www.johnferald.net/TFP>.
- Flood, Sarah, Miriam King, Renae Rodgers, Steven Ruggles, Robert Warren, and Michael Westberry. 2022. "Integrated Public Use Microdata Series, Current Population Survey: Version 10.0 [dataset]. Minneapolis, MN: IPUMS." <https://doi.org/10.18128/D030.V10.0> .
- Fujita, Shigeru, Giuseppe Moscarini, and Fabien Postel-Vinay. 2020a. "Measuring Employer-to-Employer Reallocation." *NBER Working Paper* .
- . 2020b. "Measuring Employer-to-Employer Reallocation: Dataset." *NBER Working Paper* URL <https://campuspress.yale.edu/moscarini/data/>.
- Fujita, Shigeru and Garey Ramey. 2009. "The Cyclicity of Separation and Job Finding Rates." *International Economic Review* 50 (2):415–430.
- Galí, Jordi and Thijs Van Rens. forthcoming. "The Vanishing Procyclicality of Labor Productivity." *The Economic Journal* .
- Gertler, Mark and Peter Karadi. 2015. "Monetary Policy Surprises, Credit Costs, and Economic Activity." *American Economic Journal: Macroeconomics* 7 (1).
- Gilchrist, Simon and Egon Zakrajšek. 2012a. "Credit Spreads and Business Cycle Fluctuations." *American Economic Review* 102 (4).
- . 2012b. "Credit Spreads and Business Cycle Fluctuations: Dataset." *American Economic Review* 102 (4). URL <https://www.openicpsr.org/openicpsr/project/112536/version/V1/view>.
- Golosov, Mikhail and Guido Menzies. 2020. "Agency Business Cycles." *Theoretical Economics* 15 (1):123–158.
- Gomez, Victor, Agustin Maravall, and Daniel Pena. 1999. "Missing Observations in ARIMA Models: Skipping Approach versus Additive Outlier Approach." *Journal of Econometrics* 88 (2):341 – 363.
- Gorodnichenko, Yuriy and Michael Weber. 2016. "Are Sticky Prices Costly? Evidence from the Stock Market." *American Economic Review* 106 (1):165–99.
- Gürkaynak, Refet S., Brian Sack, and Eric Swanson. 2005. "The Sensitivity of Long-Term Interest Rates to Economic News: Evidence and Implications for Macroeconomic Models." *American Economic Review* 95 (1):425–436.
- Hagedorn, Marcus and Iourii Manovskii. 2008. "The Cyclical Behavior of Equilibrium Unemployment and Vacancies." *American Economic Review* 95 (1):25–49.
- Hall, Robert. 2005. "Employment Fluctuations with Equilibrium Wage Stickiness." *American Economic Review* 95 (1):50–65.
- . 2017a. "High Discounts and High Unemployment." *American Economic Review* 107 (2):305–30.
- . 2017b. "High Discounts and High Unemployment: Dataset." *American Economic Review* 107 (2):305–30. URL <https://www.openicpsr.org/openicpsr/project/113008/version/V1/view>.
- Jolivet, Grégory, Fabien Postel-Vinay, and Jean-Marc Robin. 2006. "The empirical content of the job search model: Labor mobility and wage distributions in Europe and the US." *European Economic Review* 50 (4):877–907.
- Jurado, Kyle, Sydney Ludvigson, and Serena Ng. 2015a. "Measuring Uncertainty." *American Economic Review*

- 105 (3).
- . 2015b. “Measuring Uncertainty: Dataset.” *American Economic Review* 105 (3). URL <https://www.openicpsr.org/openicpsr/project/135741/version/V1/view>.
- Krusell, Per, Toshihiko Mukoyama, Richard Rogerson, and Aysegul Sahin. 2017. “Gross Worker Flows Over the Business Cycle.” *American Economic Review* 107 (11):3447–76.
- Lilien, David. 1982. “Sectoral Shifts and Cyclical Unemployment.” *Journal of Political Economy* 90 (4):777–793.
- Ljungqvist, Lars and Thomas Sargent. 2017. “The Fundamental Surplus.” *American Economic Review* 107 (9).
- Mercan, Yusuf and Benjamin Schoefer. 2020. “Jobs and Matches: Quits, Replacement Hiring, and Vacancy Chains.” *American Economic Review: Insights* 2 (1):101–24.
- Mitman, Kurt and Stanislav Rabinovich. 2020. “Do Unemployment Benefit Extensions Explain the Emergence of Jobless Recoveries?” *Working Paper* .
- Mortensen, Dale and Christopher Pissarides. 1994. “Job Creation and Job Destruction in the Theory of Unemployment.” *The Review of Economic Studies* 61 (3):397–415.
- Nagypál, Éva. 2008. “Worker reallocation over the business cycle: The importance of employer-to-employer transitions.” *NBER Working Paper* .
- Pissarides, Christopher A. 2009. “The Unemployment Volatility Puzzle: Is Wage Stickiness the Answer?” *Econometrica* 77 (5):1339–1369.
- Romer, Christina D. and David H. Romer. 2004. “A New Measure of Monetary Shocks: Derivation and Implications.” *American Economic Review* 94 (4):1055–1084.
- Shimer, Robert. 2005. “The Cyclical Behavior of Equilibrium Unemployment and Vacancies.” *American Economic Review* 95 (1):25–49.
- . 2012a. “Reassessing the Ins and Outs of Unemployment.” *Review of Economic Dynamics* 15 (2):127–148.
- . 2012b. “Reassessing the Ins and Outs of Unemployment: Dataset.” *Review of Economic Dynamics* 15 (2):127 – 148. URL <https://sites.google.com/site/robertshimer/research/flows>.
- Silva, Jose and Manuel Toledo. 2013. “The Unemployment Volatility Puzzle: The Role of Matching Costs Revisited.” *Economic Inquiry* 51 (1):836–843.
- Survey, of Income and Program Participation (SIPP) [dataset]. NBER Public Use Data. URL <https://www.nber.org/research/data/survey-income-and-program-participation-sipp>.
- Tjaden, Volker and Felix Wellschmied. 2014. “Quantifying the Contribution of Search to Wage Inequality.” *American Economic Journal: Macroeconomics* 6 (1):134–61.
- Uhlig, Harald. 2005. “What are the Effects of Monetary Policy on Output? Results from an Agnostic Identification Procedure.” *Journal of Monetary Economics* 52 (2):381–419.
- Wieland, Johannes and Mu-Jeung Yang. 2020a. “Financial Dampening.” *Journal of Money, Credit and Banking* 52 (1):79–113.
- . 2020b. “Financial Dampening: Dataset.” *Journal of Money, Credit and Banking* 52 (1):79–113. URL <https://www.openicpsr.org/openicpsr/project/112951/version/V1/view>.